1968

Drain Modulation of the Field-effect Transistor Amplifier

John C. Lietz

121

DRAIN MODULATION OF THE

FIELD-EFFECT TRANSISTOR AMPLIFIER

BY

JOHN C. LIETZ

A thesis submitted
in partial fulfillment of the requirements for the
degree Master of Science, Department of
Electrical Engineering, South Dakota
State University

January, 1968

DRAIN MODULATION OF THE

FIELD-EFFECT TRANSISTOR AMPLIFIER

This thesis is approved as a creditable and independent investigation by a candidate for the degree, Master of Science, and is acceptable as meeting the thesis requirements for this degree, but without implying that the conclusions reached by the candidate are necessarily the conclusions of the major department.

Thesis Advisor Date

Head, Electrical Engineering Department Date

2661-9

ACKNOWLEDGMENTS

The author wishes to express his appreciation and gratitude to Dr. F. C. Fitchen, whose guidance and advice made this investigation possible, and to the National Science Foundation for financial support of this investigation.

J.C.L.
M.H.G.

TABLE OF CONTENTS

LIST OF TABLES

LIST OF FIGURES

CHAPTER I

INTRODUCTION

Rapid transmission of information from one point to another is extremely vital to our modern society. Millions of messages are transmitted each day through a variety of communication systems. A large majority of these systems rely upon some type of modulation process.

The word "modulate" did not originate in the communications field. Like many other terms it was adopted because it aptly described the process to which it is now commonly associated. Basically the term means: to adjust; to regulate; to change; to alter; to vary; or to inflect as with the voice. For example, speaking and singing are both modulation processes where sound is varied in such a manner as to convey information. In a more technical sense, modulation is impressing an intelligence signal upon a carrier signal that is constant in all respects. The desired result of this combination is an information-bearing signal that is easily transmitted over long distances through an available medium.

When the transmission medium is the earth's atmosphere, the carrier signal is usually a sinusoidal radio frequency (RF) wave that is constant in both magnitude and frequency. In modulating this carrier one of its characteristics or parameters must be varied in accordance with the intelligence signal, more commonly referred to as the modulating signal. The two characteristics of a continuous RF wave that can be varied are the magnitude and the angle. From this it is obvious that there are two basic types of modulation available. The term "amplitude modulation" (AM) is used to describe the process where the magnitude of the RF wave is modulated, and the term "angle modulation" is associated with modulating the angle of the RF wave. Angle modulation can be further broken down into phase modulation (PM) and frequency modulation (FM) which are very closely related. Phase modulation results from varying the phase angle of the RF wave; while frequency modulation is produced by varying the instantaneous frequency of the RF wave.

Early attempts to produce a modulated wave were concerned mainly with amplitude modulation. However, some experimenters, such as Fressenden, approached the problem by first varying the frequency of the RF wave. They theorized that this varying frequency wave would then be amplitude modulated when applied to a tuned circuit because it would cause the circuit to move in and out of resonance. In essence, the main objective was amplitude modulation.[12]

Many difficulties plagued the early experimenters. The first major problem was to develop a reliable, low-noise, RF generator. Originally a spark system was used where spark rates as high as 10,000 Hz were attained. However, due to the high noise level in such systems, it was soon realized that sustained wave generators would be necessary. It was in the early 1900's that Alexanderson and his associates developed high-frequency generators. Soon thereafter generators of suitable quality were available, and the attention switched to an efficient means of modulating the RF wave.

Up to this point a carbon button microphone had been in widespread use as the modulating element. It was usually inserted in series with the RF source or in the antenna circuit where its variable resistance characteristic modulated the RF wave. However, with the newly developed generators, it was found that the microphone would not handle the increased power levels. Several methods of modulation were tried such as placing a number of microphones in parallel, providing a cooling system for the microphone, and developing various types of liquid microphones. Many of these systems produced good results, but with the advent of DeForest's vacuum tube they were slowly abandoned.[12]

First attempts with the vacuum tube followed the previous lines of thought. It seemed logical to use the tube as a variable resistance, thereby replacing the troublesome microphone. It was then that Colpitts developed a vacuum-tube oscillator which was later modulated by inserting the modulating signal into the grid circuit. This was found to be a very practical system, and it led to other methods such as inserting the modulating signal into the plate circuit.[12] From this point on, further developments were mainly attained by improvements in the vacuum tube itself.

The invention of the bipolar transistor in 1948 signaled the start of a new era in electronics. Shortly thereafter it invaded the vacuum tube world providing smaller and more reliable circuits. Modulators were not an exception. The theory of modulation developed previously was successfully applied to the new device. Although the high power levels reached by vacuum tubes could not be achieved, other advantages such as compactness and portability made transistor modulators very attractive. Soon a complete family of transistor modulators, similar in design to the vacuum-tube modulators, was developed.

Paralleling the development of amplitude modulation we find a less enthusiastic effort in the earlier years to produce a frequency modulated wave. Originally it was thought that the bandwidth required for FM was less than that required for AM, and serious thought was given to FM development. Then in 1922 J. R. Carson pointed out that FM would not allow a narrower band to be used, but, on the contrary, it might require a wider band. His studies further led him to believe that FM produced an inherent distortion in the signal. With these conclusions the outlook for FM was very discouraging. However it did not remain this way for long. E. H. Armstrong discovered that utilizing a wider bandwidth in conjunction with the use of a limiter resulted in a reduction of noise that was not possible in AM. Thus FM found its place in modulation systems and is in widespread use today.

Although FM is superior to AM in many respects, the disadvantage of the wider bandwidth still exists. As a result of this fact, AM is still commonly used, especially where bandwidth limitations are important. Special methods of amplitude modulation have been developed in an effort to further reduce the necessary bandwidth. One such method has been to transmit only one sideband of the amplitude modulated wave and has been appropriately called single-sideband amplitude modulation (SSAM). In this way the bandwidth is effectively halved, and no loss of information is experienced because both sidebands carry the same information. Thus it is apparent that AM will continue to hold an important position in the communications field. Since there still exists a definite need for AM, efforts to improve this form of modulation must continue.

A new device that has been shown to be superior in many respects to both the vacuum tube and the bipolar transistor is the unipolar or field-effect transistor (FET). The FET has a much longer history than the bipolar transistor. Theoretically, it dates back as far as 1926 in work by J. Lilienfeld. Although not successfully constructed until recently, a patent was obtained in 1939 by O. Heil on a device which in modern terminology would be called a field-effect transistor. Until a new approach using a reverse-biased semiconductor junction as the control device was described by Shockley in 1952, the FET commanded little attention. In the following years this device was built and tested by Dacey and Ross. However it was not until 1961 that it was successfully fabricated for commercial use. 5,18

Some of the factors that make the FET very attractive for many circuit applications are high input impedance, low self-generated noise, freedom from thermal runaway, and a higher radiation tolerance. Since the FET exhibits characteristics similar to a pentode vacuum tube, it can help fill the gap where bipolar transistors fall short of electron tubes. In addition it can function in applications where the bipolar transistor has already been used and can usually perform more satisfactorily.

The next logical step would be to apply the amplitude modulation theory to the FET in an attempt to produce a high quality modulated wave. It is the objective of this paper to analyze the FET in this application. Particular attention is given to the level of distortion in the modulated wave and to the percent modulation relative to the magnitude of the modulating signal. The effect of the static bias conditions is also investigated. A mathematical analysis in these areas of study is made using a second order polynomial in v_{DS} (drain-source voltage) to represent the voltage transfer characteristic. Deviations from the predicted results are justified using an arctangent representation of the input-output characteristic for large-signal conditions.

This study includes the amplifier classes A, B, and C. In addition to several small-signal FETs, a presently available power FET is also considered.

CHAPTER II

AMPLITUDE MODULATION

A. Mathematical Representation of the Modulated Waveform

Amplitude modulation was defined in the previous chapter as varying the magnitude of a sinusoidal RF carrier wave in proportion to the amplitude of an intelligence signal. For simplicity and ease of investigation, the intelligence or modulating signal can be represented by a sinusoidal waveform of constant amplitude and frequency given by

$$V_a \sin \omega_a t$$

In this expression V_a is the peak magnitude and ω_a is the angular frequency of the modulating waveform. In practice the angular frequency is usually in the audio frequency range and is much smaller than the angular frequency of the RF carrier. Similarly the RF carrier can be represented mathematically by

$$V_{co} \sin \omega_c t$$

Here again the peak magnitude is given by V_{co}, and the angular frequency is ω_c. If this waveform is to be amplitude modulated, it will be necessary to vary the magnitude V_{co} in accordance with the modulating wave. Therefore the amplitude of a modulated RF wave can be represented by

$$V_{co} + kV_a \sin \omega_a t$$

where k is a constant of proportionality. The complete mathematical expression for an amplitude modulated wave then becomes

$$v(t) = (V_{co} + kV_a \sin \omega_a t)\sin \omega_c t \qquad (2\text{-}1)$$

This is shown graphically in Fig. 1. There we see that the envelope of the modulated wave is a sinusoid whose frequency is equal to the frequency of the modulating wave. In other words, the amplitude of the RF wave is varying proportionally with the modulating wave.

B. Percent Modulation of an Amplitude Modulated Wave

The deviation of the carrier amplitude due to modulation can be expressed as a percentage of the unmodulated carrier amplitude. Let Eq. (2-1) be rewritten in the form:

$$v(t) = V_{co}(1 + \frac{kV_a}{V_{co}} \sin \omega_a t) \sin \omega_c t \qquad (2\text{-}2)$$

The ratio kV_a/V_{co} gives the fractional deviation of the carrier from its unmodulated value. This ratio is commonly called the modulation factor and is given the designation:

$$m = \frac{kV_a}{V_{co}} \qquad (2\text{-}3)$$

When multiplied by 100 percent this becomes the percentage modulation. Thus the modulation factor gives the fractional extent to which the amplitude of the carrier is varied.

Considering Fig. 1, it is seen that the product mV_{co} gives the actual deviation of the carrier from its unmodulated value in

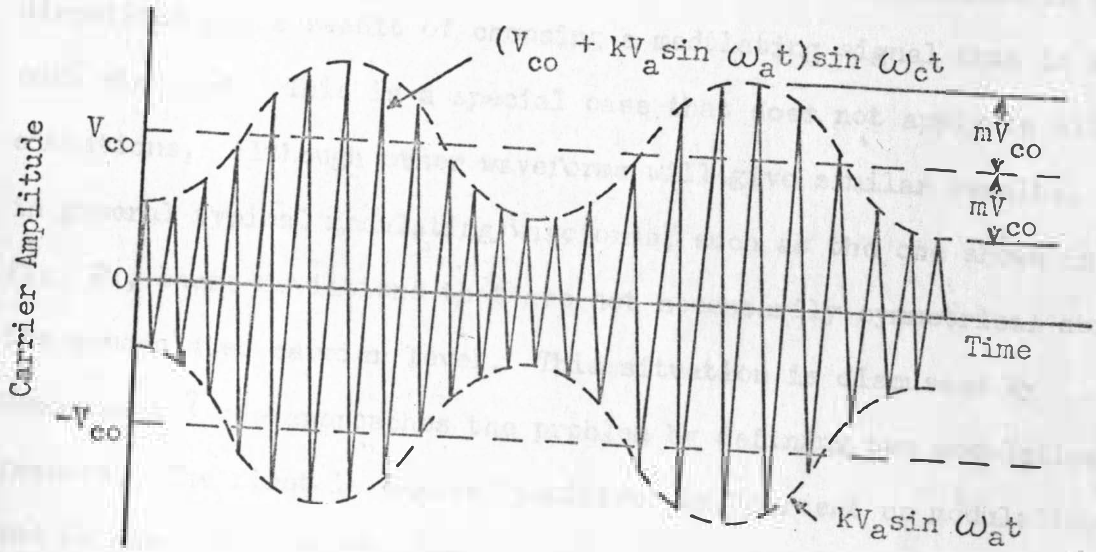

Fig. 1. Amplitude modulated wave with sinusoidal modulation.

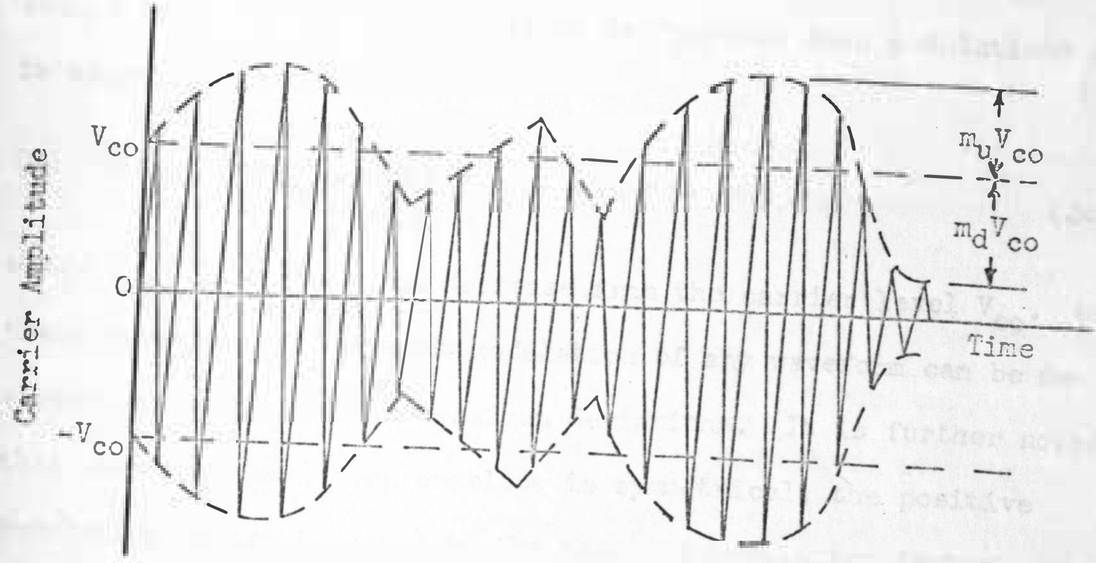

Fig. 2. Amplitude modulated wave with nonsymmetrical modulation.

both positive and negative directions. The equal deviations in both directions are a result of choosing a modulating signal that is a pure sinusoid. This is a special case that does not apply to all situations. Although other waveforms will give similar results, in general typical modulating waveforms, such as the one shown in Fig. 2., cause deviations that are not necessarily symmetrical about the unmodulated carrier level. This situation is discussed by Gaudernack.[7] He approaches the problem by defining two modulation factors. The first is called "positive" or "percent up modulation" and is given by the relation

$$m_u = \frac{V_{max}}{V_{co}} \qquad (2\text{-}4)$$

where V_{max} is the maximum increase from the carrier level V_{co}. The second factor is called "negative" or "percent down modulation" and is expressed as

$$m_d = \frac{V_{min}}{V_{co}} \qquad (2\text{-}5)$$

where V_{min} is the maximum decrease from the carrier level V_{co}. Using these relations the percent modulation of any waveform can be described in terms of their maximum deviations. It is further noted that when the modulation envelope is symmetrical, the positive modulation factor is equal to the negative modulation factor. However, if experimental evidence shows the modulation to be symmetrical, it cannot be concluded that the envelope is free from harmonics.

Again referring to Fig. 1, it is obvious that the modulation cannot exceed 100 percent. To exceed this level would imply reduction of the carrier to a level less than zero. This is clearly not realizable. However, if a nonsymmetrical modulation envelope is assumed, this limitation is partially eliminated. Although the negative modulation is still limited to 100 percent, it is now theoretically possible to achieve positive modulation factors above this level. The limitation on the positive modulation is then determined by the characteristics of the modulating device.

As indicated previously, the modulating waveform that is usually used for experimental investigation is the sine wave. This will result in symmetrical modulation provided that the modulator does not introduce any nonlinearities. Therefore with this waveform either the positive or negative deviations can be measured to determine the percent modulation.

C. Sideband Frequencies in an Amplitude Modulated Wave

The early experimenters did not know of the existence of sideband frequencies in an amplitude modulated wave. Some of them did discuss the possibility that a tuned circuit might resist a rapid change in the amplitude of the carrier as would be encountered with the higher voice frequencies. However no particular solutions to this problem were formulated. The actual discovery of sideband frequencies has been credited to Carl Englund in 1914. It appears that he first set up the amplitude modulation equation which led to their discovery.[12]

Mathematically, the existence of sidebands is demonstrated by applying the trigonometric relation

$$\sin x \sin y = \tfrac{1}{2}\left[\cos(x - y) - \cos(x + y)\right] \qquad (2\text{-}6)$$

to Eq. (2-2). This substitution gives frequency components consisting of the carrier frequency and the sum and difference frequencies of the carrier and modulating signals as shown in the following equation:

$$v(t) = V_{co}\sin \omega_c t + \frac{mV_{co}}{2}\Big[\cos(\omega_c - \omega_m)t - \cos(\omega_c + \omega_m)t\Big] \qquad (2\text{-}7)$$

Here m is the same as that defined in Eq. (2-3). This equation is represented graphically in the frequency spectrum of Fig. 3. Also shown for reference is the modulating frequency ω_a. The frequency components $(\omega_c - \omega_a)$ and $(\omega_c + \omega_a)$ are the sidebands that are generated in the modulation process. The amplitudes of these sidebands are equal to $\pm V_{co}/2$ which indicates a direct relationship to the percent modulation and the unmodulated carrier amplitude. Thus we see that the width of the frequency band required for the modulated wave is equal to twice the highest modulating frequency. This imposes the requirement on the modulator that its bandwidth must be at least twice the highest expected modulating frequency. If this is not observed, the sidebands furthest from the carrier will be attenuated, and the resulting intelligence signal will be distorted when the wave is demodulated at the receiving end.

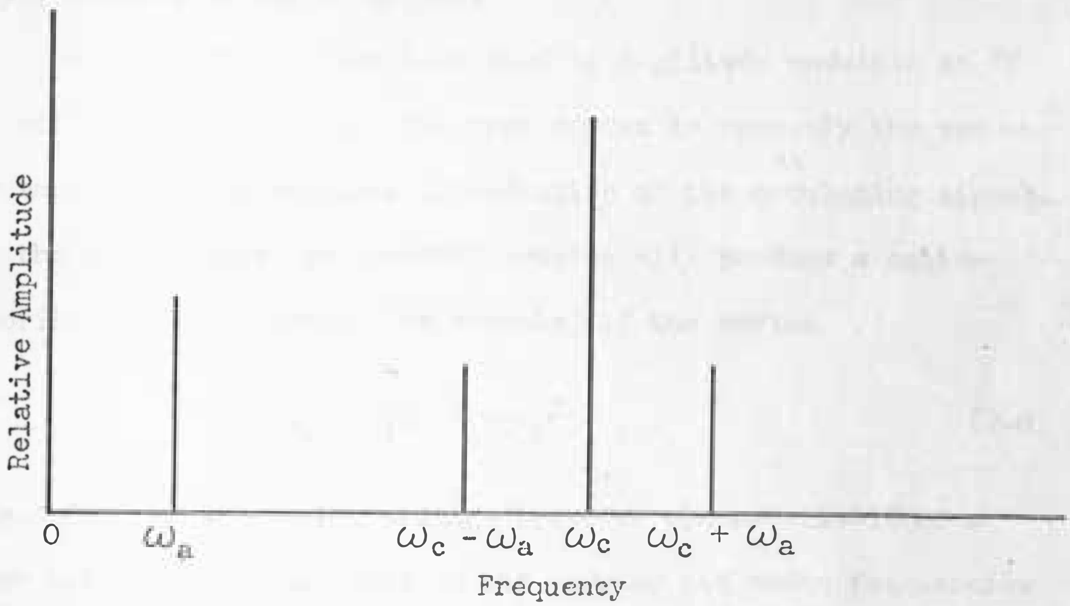

Fig. 3. Frequency spectrum of an amplitude modulated wave.

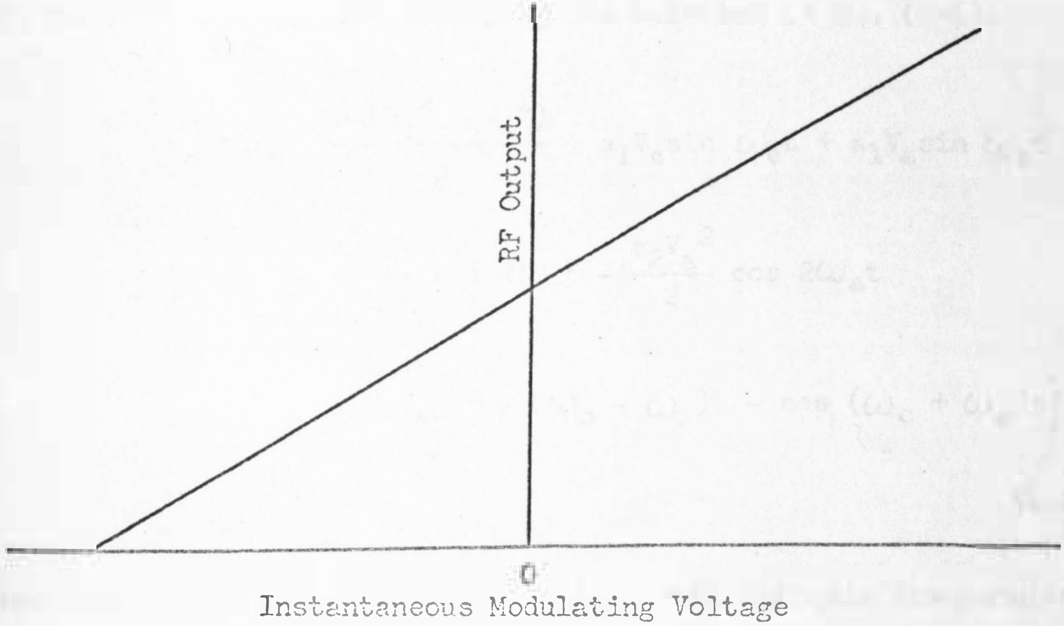

Fig. 4. Modulation characteristic of an ideal modulator.

D. The Modulation Characteristic

Several methods have been used to amplitude modulate an RF wave with various results. The most common is probably the vacuum tube amplifier. Appropriate introduction of the modulating signal into the grid, plate, or cathode circuits will produce a satisfactorily modulated wave. For example, if the series

$$v_o = a_o + a_1 v_i + a_2 v_i^2 + \ldots \qquad (2\text{-}8)$$

is used to approximate the voltage transfer characteristic of a common cathode amplifier, and if the carrier and audio frequencies are inserted at the input

$$v_i = V_c \sin \omega_c t + V_a \sin \omega_a t \qquad (2\text{-}9)$$

the result will be, after applying the relation in Eq. (2-6):

$$\begin{aligned} v_o = a_o &+ \frac{a_2(V_c^2 + V_a^2)}{2} + a_1 V_c \sin \omega_c t + a_1 V_a \sin \omega_a t \\ &- \frac{a_2 V_c^2}{2} \cos 2\omega_c t - \frac{a_2 V_a^2}{2} \cos 2\omega_a t \\ &+ a_2 V_c V_a \left[\cos(\omega_c - \omega_a)t - \cos(\omega_c + \omega_a)t\right] \\ &+ \ldots \end{aligned} \qquad (2\text{-}10)$$

Thus a modulated wave is generated along with harmonic frequencies of both the carrier and the audio frequencies. These undesired harmonics, however, can be filtered out with appropriate circuitry.

If the next term in the series had been considered, sideband frequencies of ($\omega_c - 2\omega_a$) and ($\omega_c + 2\omega_a$) would have been generated. These terms produce distortion in the modulated wave that cannot be practically filtered out. Therefore we see that the desired characteristic of a modulator is as shown in Fig. 4. The amplitude of the RF output must vary in direct proportion to the instantaneous modulating signal. Any distortion terms that cannot be filtered out through an appropriate amplifier design are the result of a curvature in this modulation characteristic.

In the particular case of plate modulation, the modulation characteristic is easily obtained. A plot of the amplitude of the RF output as a function of the steady state supply voltage that is in series with the modulating input, as outlined by Gray, is a good representation.[10] Using this technique, a rapid evaluation of the modulator performance can be obtained.

The requirements on the level of distortion are becoming very strict due to the number and power of broadcast stations and the desire for increased fidelity. As a result, the distortion should not exceed a few percent in the worst case.[16]

E. Modulator Power Output

Since power output is an important factor in determining the strength of the transmitted signal as well as modulator efficiency, one is concerned with measuring this quantity. If the load into which the modulator is operating is known, a knowledge of the RMS value of the modulated voltage wave is sufficient to determine the output power.

The RMS value of the wave given in Eq. (2-1) is easily calculated and is given by

$$V_{RMS} = \frac{V_{co}}{2}\sqrt{2 + m^2} \tag{2-11}$$

Therefore a knowledge of the peak value of the unmodulated carrier output and the modulation factor are sufficient for determining the RMS value of the modulated wave. Since both are easily measured, no problem is encountered.

Combining the result of Eq. (2-11) with the value of the modulator load (R_L), the power output is obtained:

$$P = \frac{{V_{RMS}}^2}{R_L} \quad \frac{{V_{co}}^2(2 + m^2)}{4R_L} \tag{2-12}$$

As might be expected, the magnitude of the carrier is very important in the determination of the output power.

F. Presently Used Modulating Devices

Vacuum tubes and the bipolar transistor have both been used as modulating devices as mentioned in Chapter I. Satisfactory results have been obtained, but some difficulty has been encountered in obtaining linear results at high modulation factors. This problem has been reduced in vacuum tubes through appropriate biasing methods and insertion of the modulating signal at more than one point. On the other hand, transistors have unique difficulties with regard to both modulation depth and linearity. These seem to be caused mainly by a decrease in current gain with increase in power output and a large feedthrough capacitance found in transistors. These difficulties tend to limit the quality obtainable from compact, transistorized modulators.[9]

CHAPTER III

THE FET DRAIN MODULATOR

A. Modulating Methods Extended to the FET

Historically, three basic methods of modulating vacuum tube and transistor amplifiers have been used. In the case of the vacuum tube the modulating signal has been inserted at the grid, the cathode, and the plate with varying degrees of success. Similarly, with the bipolar transistor the signal has been introduced at the base, the emitter, and the collector -- each resulting in satisfactory modulation. Each method has some advantage relative to the others in regard to any particular application.

Since the FET is an active device quite similar to the pentode vacuum tube, one might consider it in similar roles. Modulation could conceivably result from introduction of the modulating signal at the gate, the source, or the drain. Each case constitutes a complete study in itself. For the present investigation, only the drain case will be considered. This method allows the largest variety in regard to the various classes of amplifiers available for use.

B. The Field Effect Transistor

The FET is basically a three terminal device. The control electrode, commonly referred to as the gate, is in close proximity to a conducting channel. This is illustrated in Fig. 5 for the

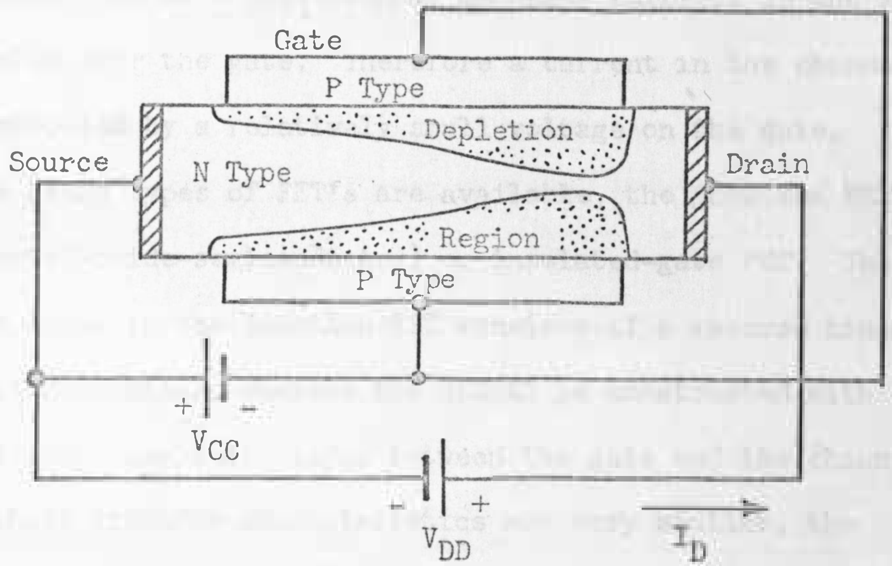

Fig. 5. Pictorial sketch of the junction FET and its appropriate biasing.

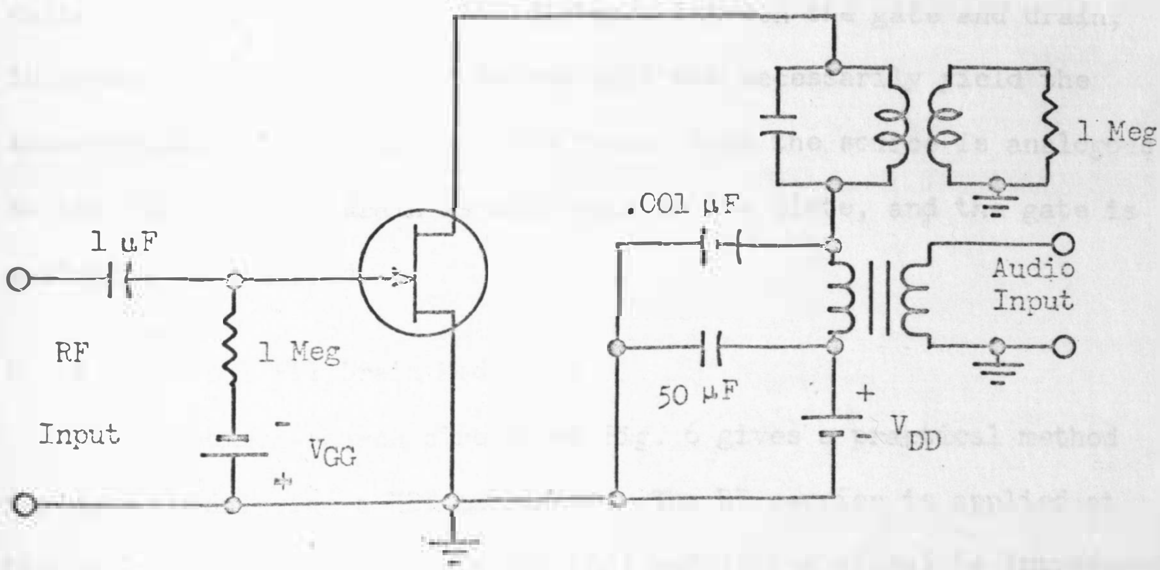

Fig. 6. A common-source, drain modulated, FET amplifier.

junction FET. A voltage on the gate will change the conductance of the channel due to a depletion of majority carriers in the channel in the region near the gate. Therefore a current in the channel can be controlled by a relatively small voltage on the gate.

Two basic types of FET's are available, the junction FET and the MOS (metal-oxide-semiconductor) or insulated-gate FET. The insulating layer in the junction FET consists of a reverse biased semiconductor junction; whereas the MOSFET is constructed with a silicon dioxide insulating layer between the gate and the channel. Although their transfer characteristics are very similar, the insulated-gate type is superior in regard to input impedance because of the silicon dioxide insulating layer.

Since the physical distance between the gate and source is quite often made less than the distance between the gate and drain, interchanging the drain and source will not necessarily yield the same results. With regard to the vacuum tube the source is analogous to the cathode, the drain is analogous to the plate, and the gate is analogous to the grid.

C. A Practical FET Drain Modulator

The common-source circuit of Fig. 6 gives a practical method for drain modulating a FET amplifier. The RF carrier is applied at the gate, and the audio frequency (AF) modulating signal is introduced into the drain circuit by means of a transformer. The tuned circuit is resonant at the carrier frequency and therefore filters the modulated wave which is available from drain to ground. The FET could be represented by its small-signal equivalent with the transconductance (g_m) and the drain resistance (r_{ds}) as significant parameters. However, since the drain voltage will vary from zero to twice V_{DD} for 100 percent modulation, both g_m and r_{ds} will vary through wide ranges. More specifically, large-signal conditions will exist for which an equivalent circuit cannot be determined.

Instead of focusing our attention on the transistor itself, consideration of the complete amplifier reveals a much more simplified approach. In this case the appropriate representation becomes the forward voltage-transfer ratio or voltage gain, the ratio of output voltage at the drain to the input voltage at the gate. Further study reveals that a plot of voltage gain as a function of V_{DS} will actually be the modulation characteristic discussed in Chapter II.

Theoretical behavior of the FET drain modulator can be predicted if the voltage-transfer ratio is represented by

$$\frac{v_{ds}}{v_{gs}} = b_o v_{DS} + c_o v_{DS}^2 \qquad (3\text{-}1)$$

For an N-channel FET v_{DS} will be positive; therefore, b_o will be negative due to the inherent phase reversal of the common-source amplifier. From experimental data c_o is usually found to be a positive quantity.

Since the modulating signal is inserted in series with the drain bias supply, the total drain voltage will be the sum of the

AF modulating signal and the d-c drain voltage:

$$v_{DS} = v(t) + V_{DS} \tag{3-2}$$

As previously discussed, the sine wave signal is most frequently used for experimental study. Therefore inserting $v(t) = V_a \sin \omega_a t$ and $v_{gs} = V_c \sin \omega_c t$ into Eqs. (3-1) and (3-2) we arrive at

$$\begin{aligned} v_{ds} &= \left(a + \frac{cV_a^2}{2}\right)V_c \sin \omega_c t \\ &+ \left(\frac{bV_aV_c}{2}\right)\left[\cos(\omega_c - \omega_a)t - \cos(\omega_c + \omega_a)t\right] \\ &- \left(\frac{cV_a^2V_c}{4}\right)\left[\sin(\omega_c + 2\omega_a)t + \sin(\omega_c - 2\omega_a)t\right] \end{aligned} \tag{3-3}$$

The following constants have been introduced to simplify the relation:

$$a = b_o V_{DS} + c_o V_{DS}^2$$

$$b = b_o + 2c_o V_{DS}$$

$$c = c_o$$

Comparing the second terms in Eqs. (2-7) and (3-3) we find that the magnitudes of the coefficients must be equal for a particular level of modulation:

$$\frac{mV_{co}}{2} = \frac{bV_aV_c}{2} \tag{3-4}$$

Also, comparing the first terms in the same two equations indicates that

$$V_{co} = (a + \frac{cV_a^{\,2}}{2})V_c \tag{3-5}$$

Substituting this into Eq. (3-4) results in an expression for the modulation factor for the drain modulator:

$$m = \frac{bV_a}{a + cV_a^{\,2}/2} \tag{3-6a}$$

From Eq. (3-3) we see that a good modulator would have a negligible c coefficient in its voltage-transfer ratio. If this condition exists, Eq. (3-6a) can be approximated:

$$m \cong \frac{bV_a}{a} = \frac{b_o + 2c_oV_{DS}}{b_oV_{DS} + c_oV_{DS}^{\,2}}\,V_a \tag{3-6b}$$

A negligible c would also indicate that $|b_o| \gg |2c_oV_{DS}|$ and Eq. (3-6a) can be further simplified to

$$m \cong \frac{V_a}{V_{DS}} \tag{3-6c}$$

Therefore we see that the percent modulation for a good drain modulator is directly proportional to the audio modulating signal and inversely proportional to the static drain voltage.

For a good modulator it was noted that c should be small to prevent the generation of the undesired sideband frequencies $(\omega_c \pm 2\omega_a)$. For the purposes of evaluation, the ratio of the undesired side frequency to the desired side frequency can be considered:

$$\lambda = \frac{c}{2b} V_a \tag{3-7}$$

Minimization of this term is desirable. Therefore a good modulator will have a small c coefficient and a large b coefficient.

CHAPTER IV

EXPERIMENTAL DATA AND DISCUSSION OF RESULTS

A. Junction FET Type 2N3823

The FET type 2N3823 exhibits the common-source drain characteristics shown in Fig. 7. The actual value of the gate-to-source voltage V_{GS} at the cutoff point of I_D is difficult to measure because of leakage currents. The approximate variation of I_D with V_{GS} derived by Shockley indicates a definite value does exist:

$$I_D = I_{DSS}\left(1 - \frac{V_{GS}}{V_P}\right)^2 \qquad (4\text{-}1)$$

Here the parameter I_{DSS} is defined as the drain saturation current at zero gate voltage, and the pinch-off voltage V_P is the value of V_{DS} above which the drain current remains essentially constant. Obviously if V_{GS} equals V_P, the drain current would be reduced to zero, and the cutoff voltage would be given simply as V_P. However V_P is also difficult to determine due to the lack of a precisely defined point of saturation as is evident in Fig. 7. An approximation must then be made. Tompkins has stated that accurate values of V_P can be measured if one percent of I_{DSS} is considered as the value of I_D at cutoff.[17] Using this criterion, the value of the gate-to-source voltage at cutoff is -2.45 volts for the particular 2N3823 FET considered.

The circuit of Fig. 8 was used to measure the small-signal transconductance g_m. The results of this measurement with a 5 mV,

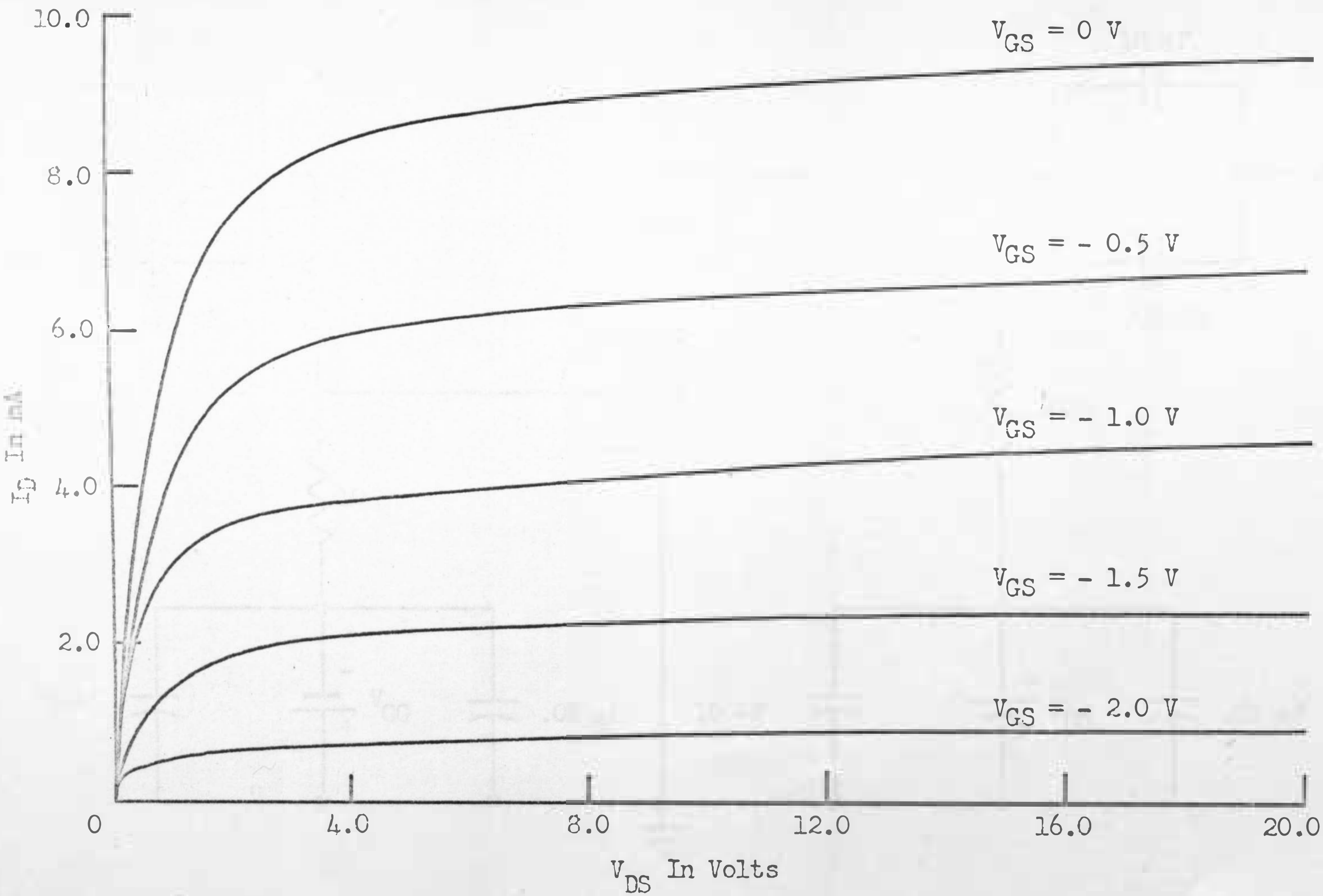

Fig. 7. Drain characteristic of the FET type 2N3823.

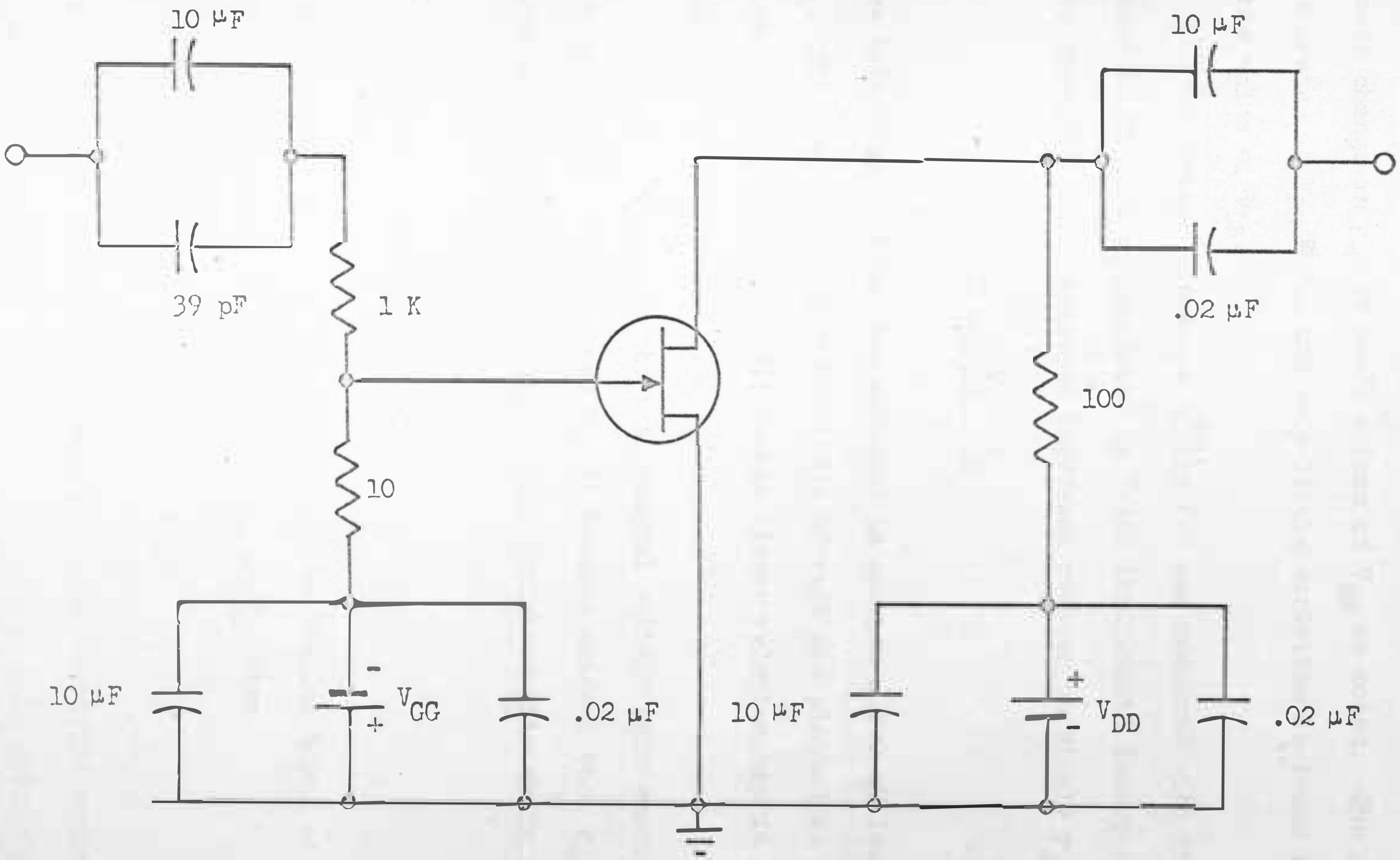

Fig. 8. FET transconductance test circuit.

1-MHz input signal at the gate are plotted in Fig. 9. A very rapid change in g_m for small values of V_{DS} is noted. The g_m virtually saturates at $V_{DS} \cong V_P$, and very little variation is found above this value of V_{DS}.

The output impedance of the FET was measured with the circuit shown in Fig. 10 as suggested by Texas Instruments Incorporated. At low frequencies the measured impedance reduces to simply r_{ds}:

$$r_{ds} = 100 \frac{V_1 - V_2}{V_2} \qquad (4\text{-}2)$$

The 1-KHz input signal was adjusted to provide a 100-mV level for V_1. The results obtained with this circuit are plotted as a function of V_{DS} in Fig. 11. A somewhat linear relationship is found to exist between r_{ds} and V_{DS}.

If one considers the small-signal voltage gain expression for an amplifier with a load R_L, it becomes evident that r_{ds} is the major contributor to the voltage gain variation with drain voltage:

$$A_V = \frac{g_m r_{ds} R_L}{r_{ds} + R_L} \qquad (4\text{-}3)$$

Also it should be noted that r_{ds} should be smaller than, or of the same order of magnitude as R_L. If $r_{ds} >> R_L$, then

$$A_V \cong g_m R_L \qquad (4\text{-}4)$$

and an extremely nonlinear voltage gain characteristic would result. It was previously noted that a plot of voltage gain versus V_{DS} is a

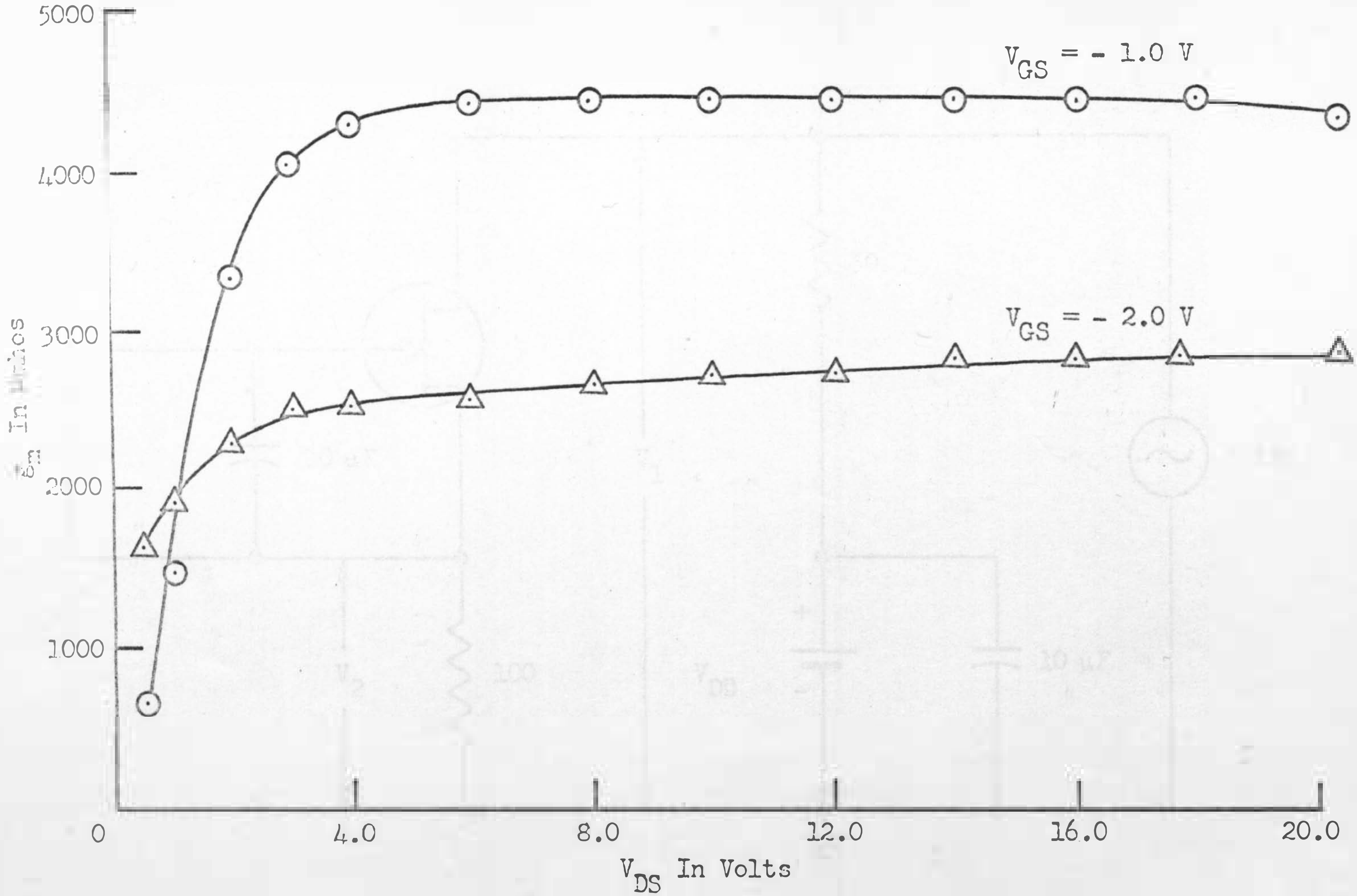

Fig. 9. Dynamic transconductance as a function of V_{DS} for the FET type 2N3823.

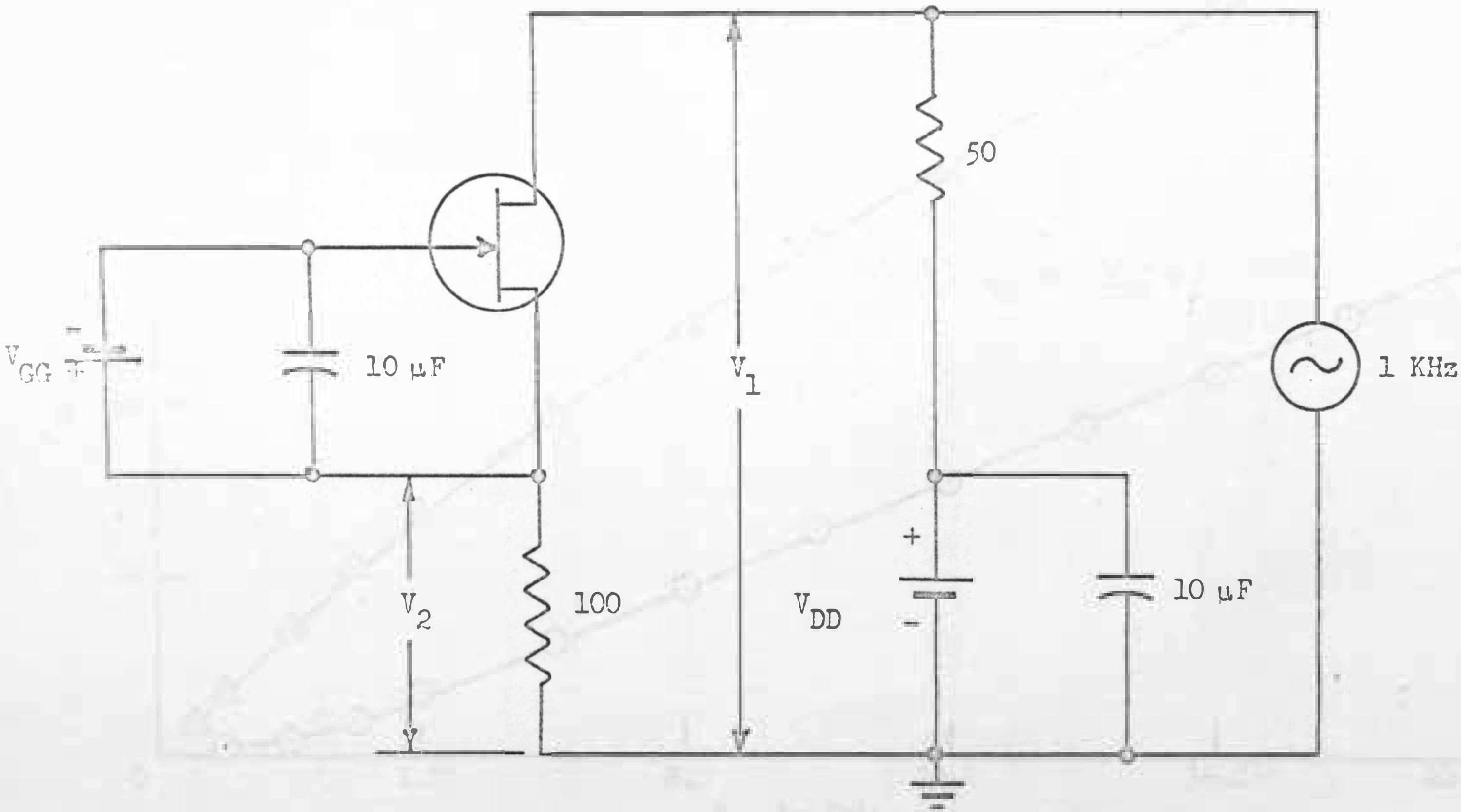

Fig. 10. FET output impedance test circuit.

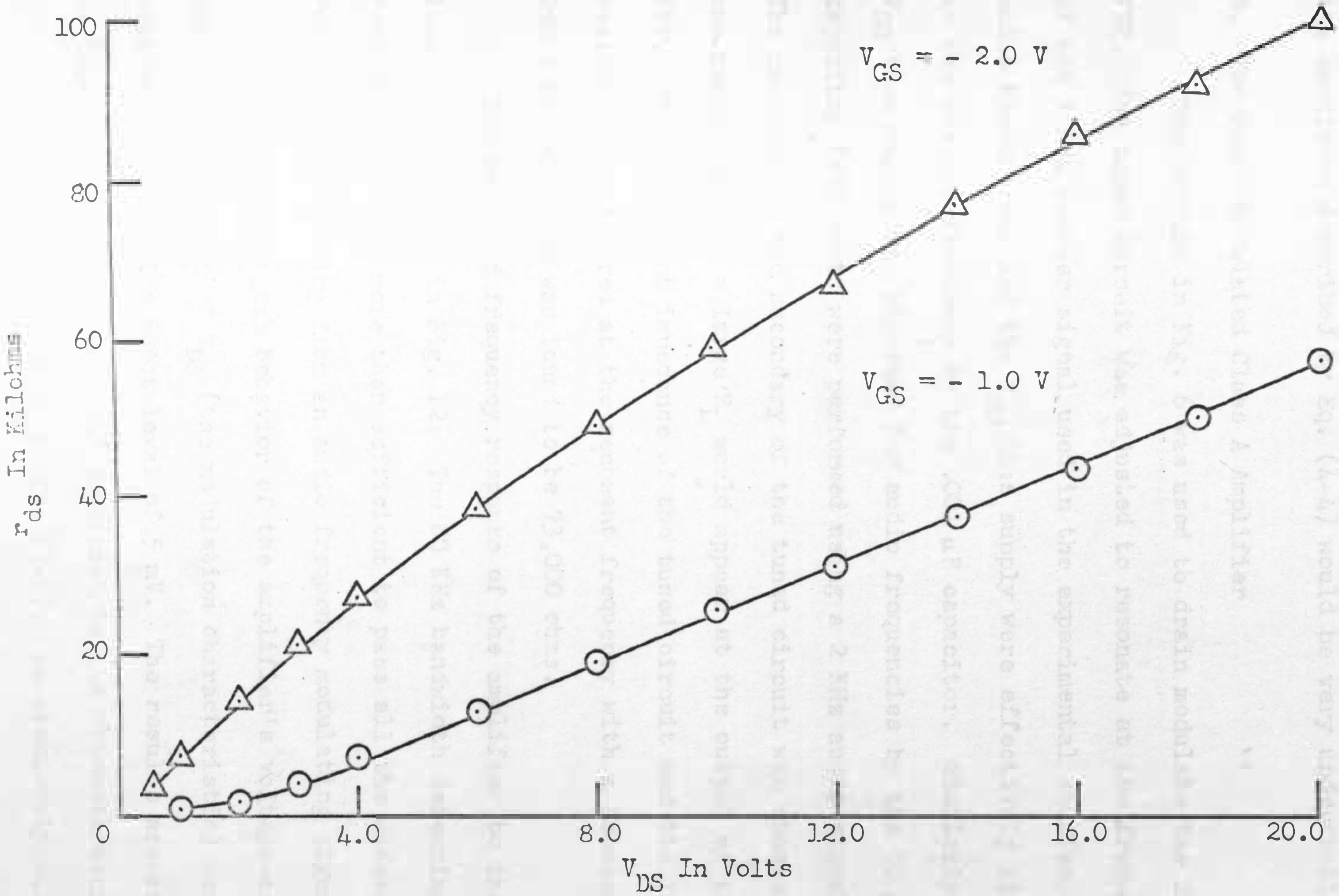

Fig. 11. Drain resistance as a function of V_{DS} for the FET type 2N3823.

good approximation for the modulation characteristic. Therefore the condition described by Eq. (4-4) would be very undesirable.

B. The Drain Modulated Class A Amplifier

The circuit in Fig. 6 was used to drain modulate the 2N3823 FET. The tuned circuit was adjusted to resonate at the frequency of the 1 MHz carrier signal used in the experimental studies. The audio transformer and the V_{DD} bias supply were effectively bipassed at the carrier frequency by the .001 μF capacitor. Similarly the V_{DD} bias supply was bipassed for audio frequencies by the 50 μF capacitor (all tests were performed using a 2 KHz audio signal). The resistor at the secondary of the tuned circuit was chosen as one megohm so that a large R_L would appear at the output of the FET. The equivalent impedance of the tuned circuit and its load resistor was measured at the resonant frequency with a Boonton Type 250-A RX meter and was found to be 73,000 ohms.

The measured frequency response of the amplifier to the RF input is displayed in Fig. 12. The 80 KHz bandwidth determined from this curve is more than sufficient to pass all the sideband frequencies resulting from an audio frequency modulating signal.

The small-signal behavior of the amplifier's voltage-transfer ratio as a function of V_{DS} (the modulation characteristic) was measured at a carrier input level of 5 mV. The results are shown in Fig. 13. The high degree of curvature in the characteristics indicates a large value of c_3 in Eq. (3-1). As previously discussed,

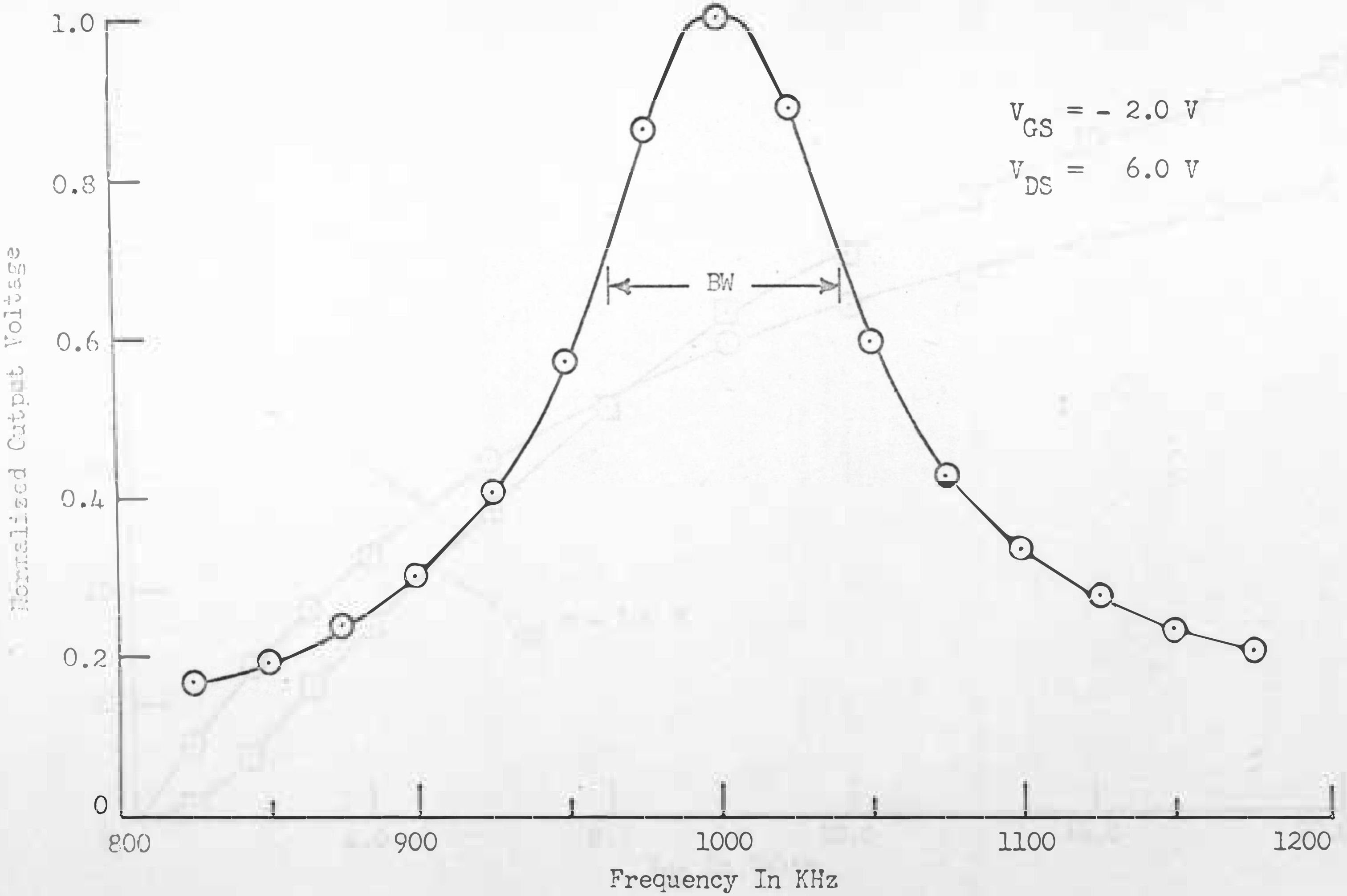

Fig. 12. Frequency response of the drain modulated amplifier of Fig. 6, FET type 2N3823.

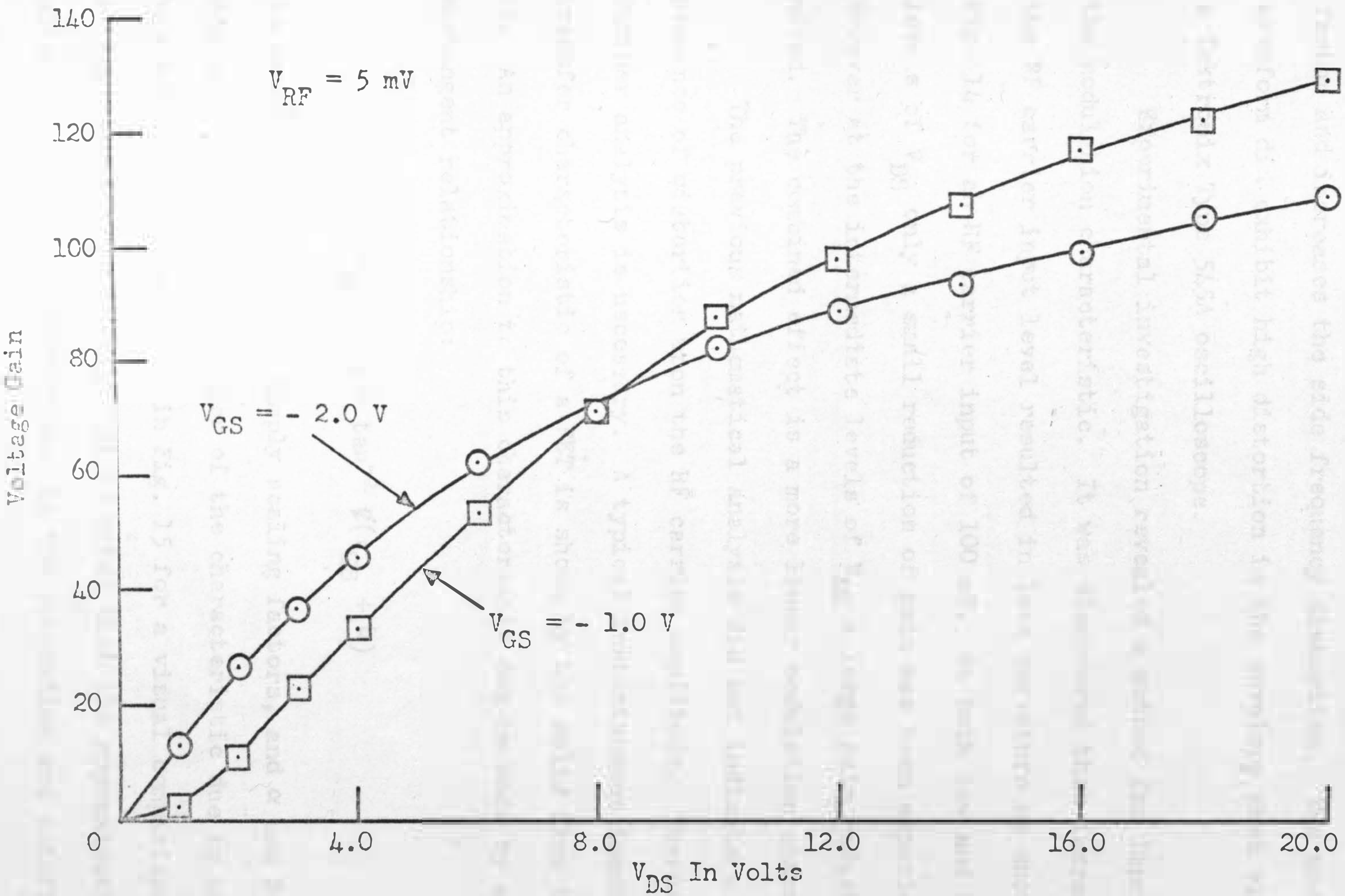

Fig. 13. Small-signal voltage gain as a function of V_{DS} for the 2N3823 FET amplifier.

this condition is undesirable because it decreases the modulation factor and increases the side frequency distortion. The modulated waveform did exhibit high distortion in the envelope when viewed on a Tektronix Type 545A oscilloscope.

Experimental investigation revealed a method for improving the modulation characteristic. It was discovered that increasing the RF carrier input level resulted in less curvature as shown in Fig. 14 for an RF carrier input of 100 mV. At both low and high levels of V_{DS} only a small reduction of gain has been experienced. However at the intermediate levels of V_{DS} a large gain reduction is noted. The combined effect is a more linear modulation characteristic.

The previous mathematical analysis did not indicate a dependence of distortion upon the RF carrier amplitude. Therefore further analysis is necessary. A typical instantaneous input-output transfer characteristic of a FET is shown by the solid line in Fig. 15. An approximation to this characteristic can be made by an arctangent relationship:

$$\theta(v_{DS} + \alpha) = \tan^{-1} \phi(v_{GS} + \beta) \qquad (4\text{-}5)$$

The constants θ and ϕ are simply scaling factors, and α and β indicate an offset from the center of the characteristic due to biasing. This relation is also given in Fig. 15 for a visual comparison with the observed characteristic. It is noted that the approximation is quite good except for differences in the saturation and cutoff regions.

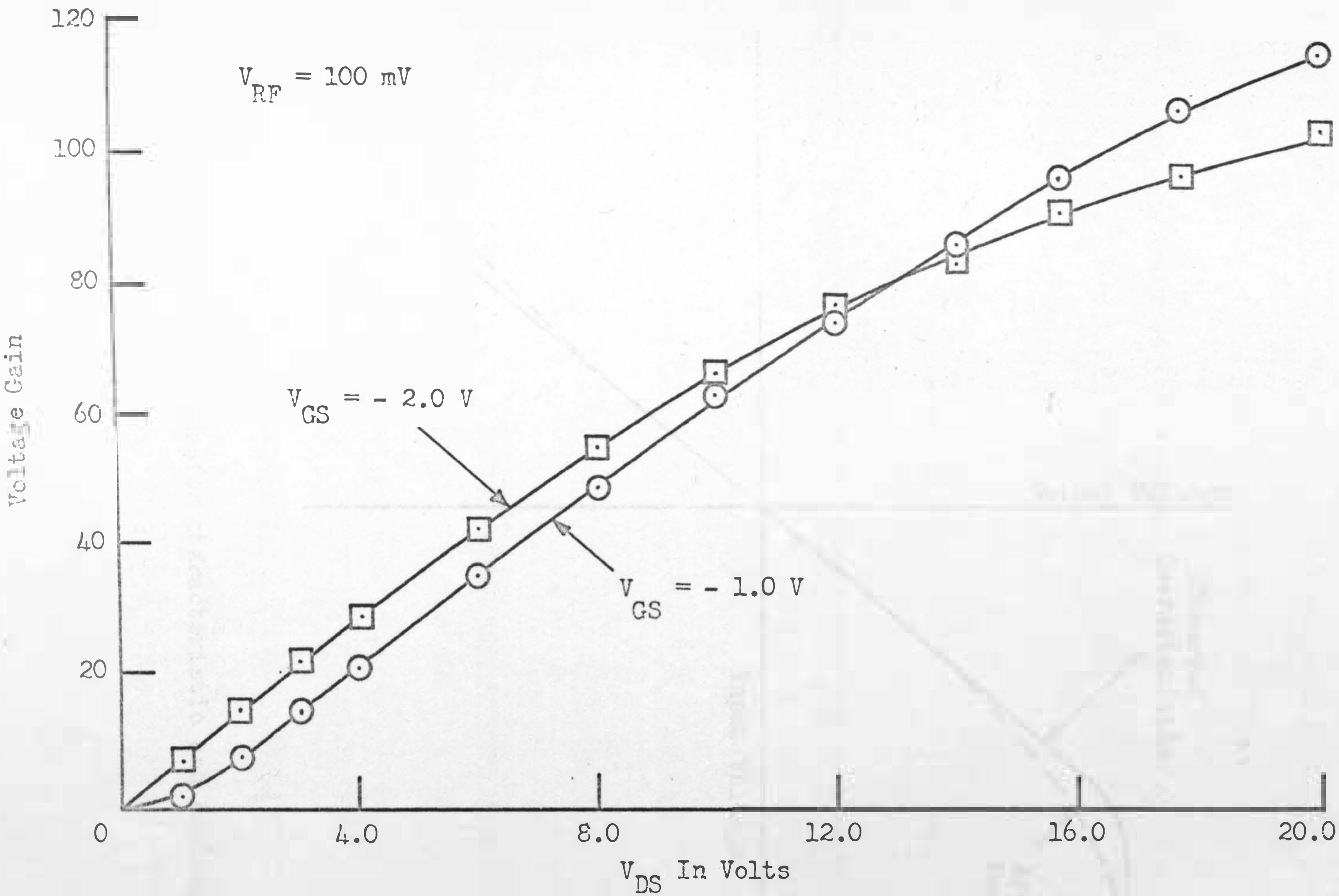

Fig. 14. Large-signal voltage gain as a function of V_{DS} for the 2N3823 FET amplifier.

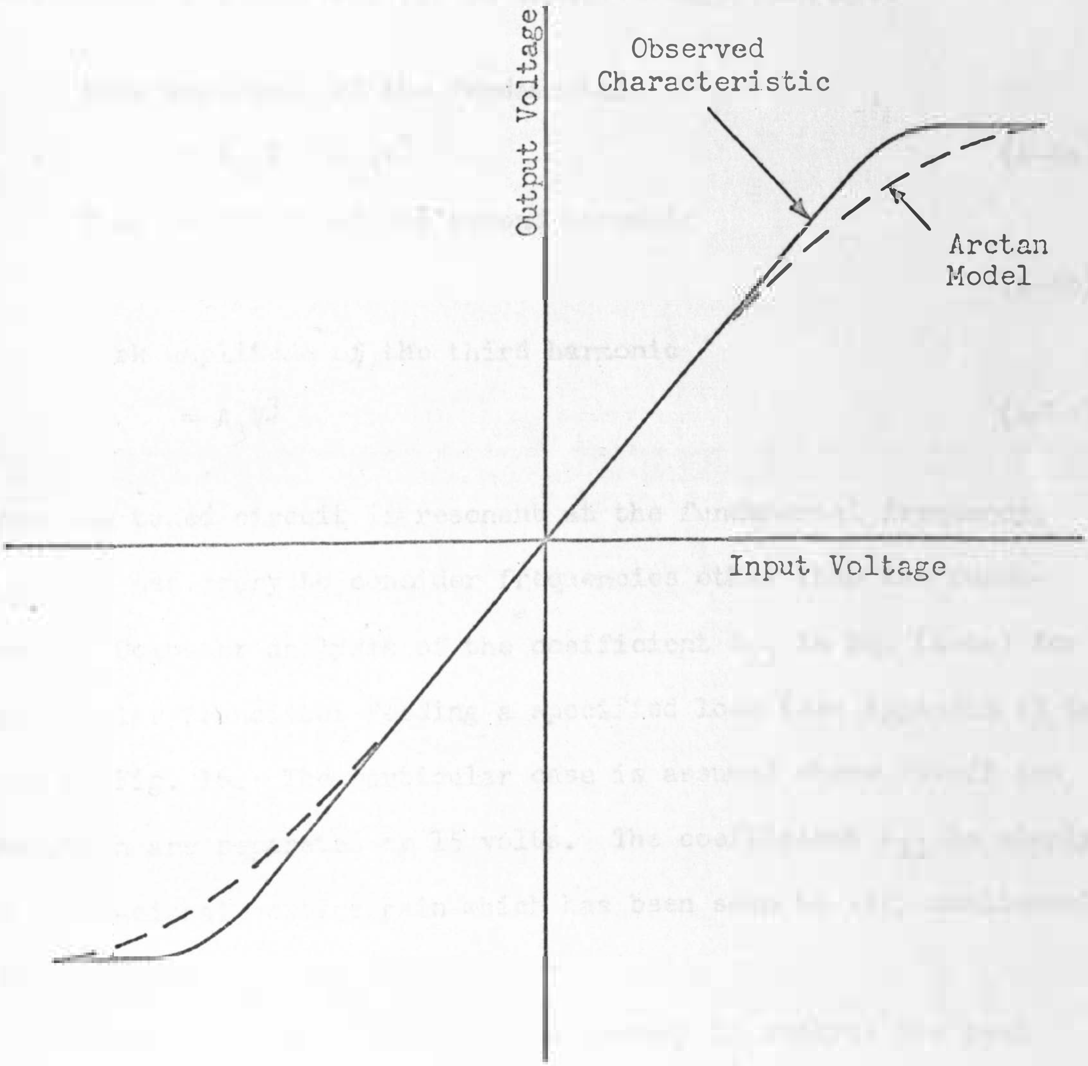

Fig. 15. Typical FET transfer characteristic and arctangent model.

The arctangent model can be analyzed in terms of a Fourier series (see Appendix A). When this is done, the following Fourier coefficients are obtained for an input voltage $V\sin\omega t$:

Peak amplitude of the fundamental

$$= A_{11}V + A_{13}V^3 \tag{4-6a}$$

Peak amplitude of the second harmonic

$$= A_2V^2 \tag{4-6b}$$

Peak amplitude of the third harmonic

$$= A_3V^3 \tag{4-6c}$$

Since the tuned circuit is resonant at the fundamental frequency, it is not necessary to consider frequencies other than the fundamental. Computer analysis of the coefficient A_{13} in Eq. (4-6a) for a particular transistor feeding a specified load (see Appendix A) is shown in Fig. 16. The particular case is assumed where cutoff and saturation are separated by 15 volts. The coefficient A_{11} is simply the small-signal voltage gain which has been seen to vary nonlinearly with V_{DS} as in Fig. 13.

We now have the information necessary to analyze the peak amplitude of the fundamental frequency component of Eq. (4-6a). The coefficient A_{11} is negative due to the 180 degree phase shift of a common-source amplifier. From Fig. 16, A_{13} is positive for intermediate values of V_{DS}. Therefore reduction in gain will result for these values of V_{DS} with a maximum reduction occuring at V_{DS} = 7.5 volts. At low and also at high levels of V_{DS} the effect on

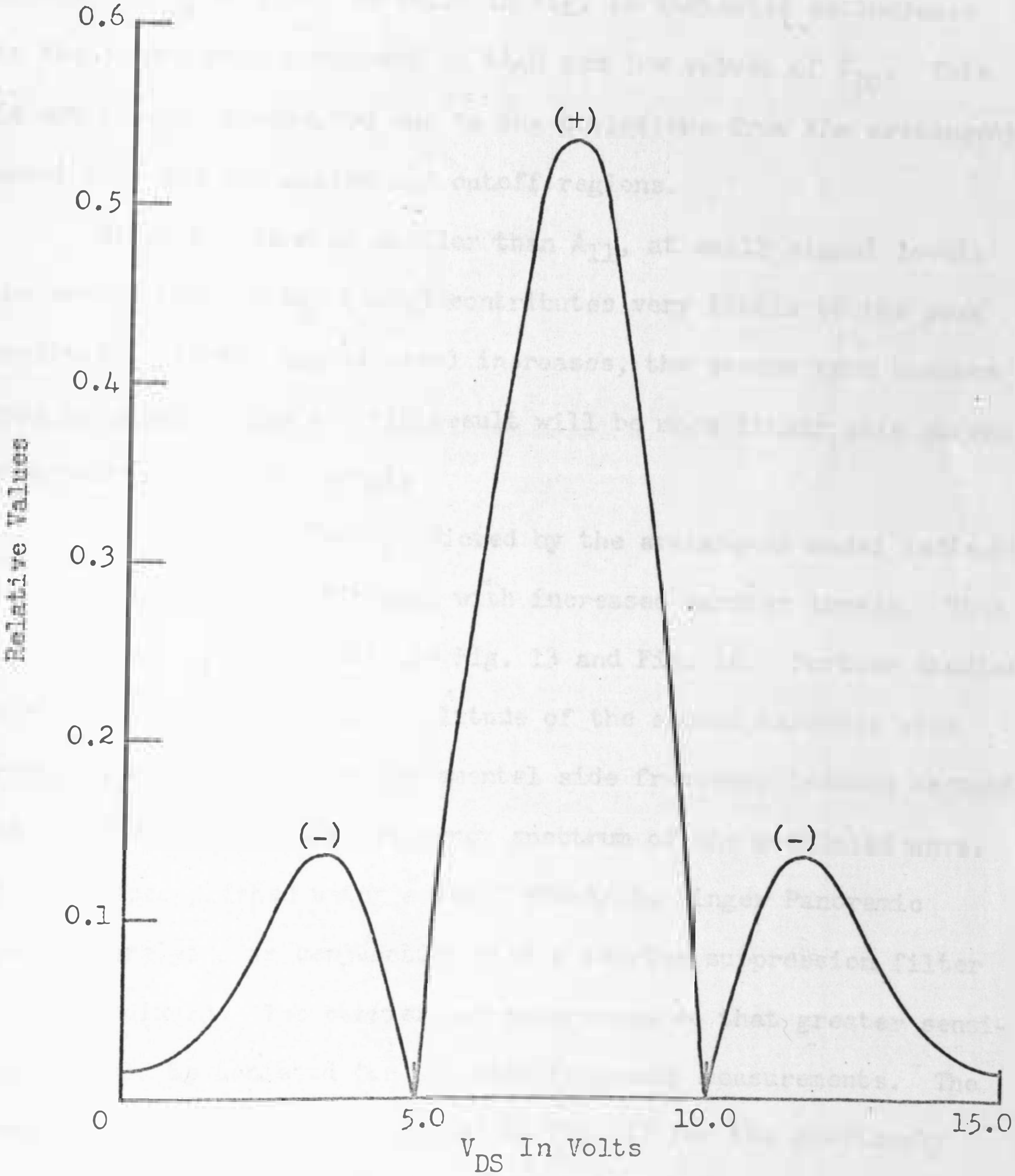

Fig. 16. Coefficient of the large-signal term in the fundamental frequency expression.

gain is not as great. This is exactly the result necessary for straightening the gain curves as previously discussed. The sign change in A_{13} at 5 and 10 volts in Fig. 16 indicates an increase in the fundamental component at high and low values of V_{DS}. This is not generally observed due to the deviations from the arctangent model near the saturation and cutoff regions.

Since A_{13} is much smaller than A_{11}, at small signal levels the second term in Eq. (4-6a) contributes very little to the peak amplitude. As the signal level increases, the second term becomes more important. The overall result will be more linear gain curves with increased input signal.

The general effect predicted by the arctangent model indicates improved modulator performance with increased carrier levels. This was observed experimentally in Fig. 13 and Fig. 14. Further studies were made by measuring the amplitude of the second harmonic side frequency relative to the fundamental side frequency (second harmonic audio distortion) in the frequency spectrum of the modulated wave. This was accomplished using a model SPA-3/25a Singer Panoramic spectrum analyzer in conjunction with a carrier suppression filter (see Appendix B). The carrier was suppressed so that greater sensitivity could be achieved for the side-frequency measurements. The results of this study are depicted in Fig. 17 for the previously discussed amplifier at 100 percent modulation. Reduction of the ratio of second harmonic side frequency to the fundamental side frequency is clearly dependent upon the RF carrier level. Test data

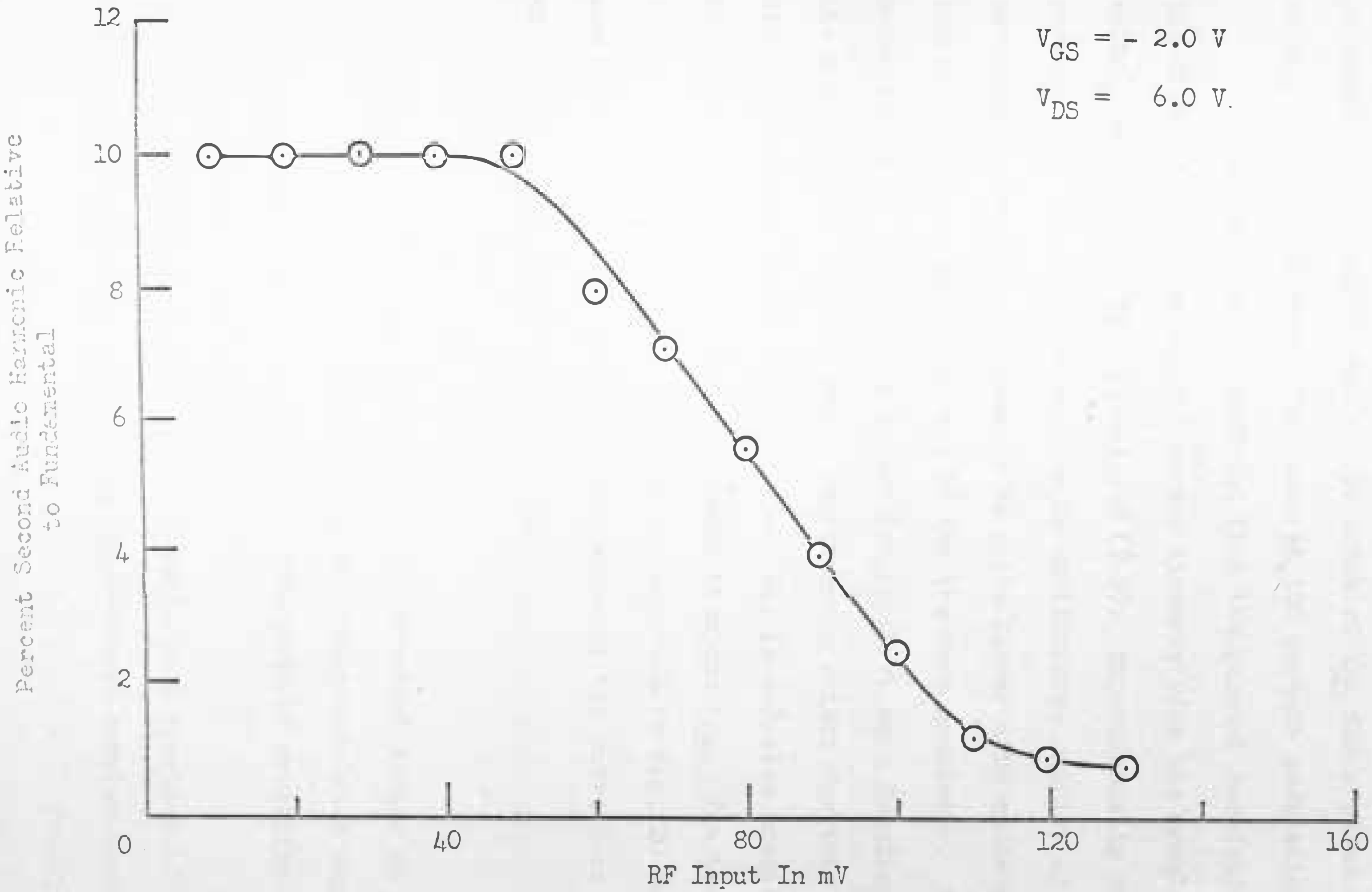

Fig. 17. Sideband distortion as a function of carrier amplitude for 100 percent modulation.

shown in Fig. 18 indicate that further optimization of this ratio is possible by choosing the proper value of V_{GS} for a given value of V_{DS}. These data were also taken at 100 percent modulation.

It was previously predicted that the percent modulation and the distortion factor would increase linearly with the modulating voltage as given by Eqs. (3-6c) and (3-7). Experimentally the percent modulation, measured from an oscilloscope display of the modulated waveform, was found to be quite linear with audio modulating voltage as shown in Fig. 19 for the test modulator. Also shown in this figure is the distortion ratio λ as a function of the audio input. A near linear relationship exists for this value also, except for large audio signals. Eq. (3-6c) also predicts an inverse relation between percent modulation and V_{DS}. The test data from the drain modulated amplifier are depicted in Fig. 20 for this particular relation. The hyperbolic shape of the curve does suggest an inverse relation between m and V_{DS}.

C. Other Operating Modes

Efficiency is quite frequently an important factor in amplifier design. To improve the efficiency of the drain modulated amplifier, class B operation can be considered. This mode of operation restricts V_{GS} to its value at cutoff.

The curves of voltage transfer ratio as a function of V_{DS} can once again be straightened by using large-signal carrier inputs as shown in Fig. 21. It appears that a 500 mV input will result in a

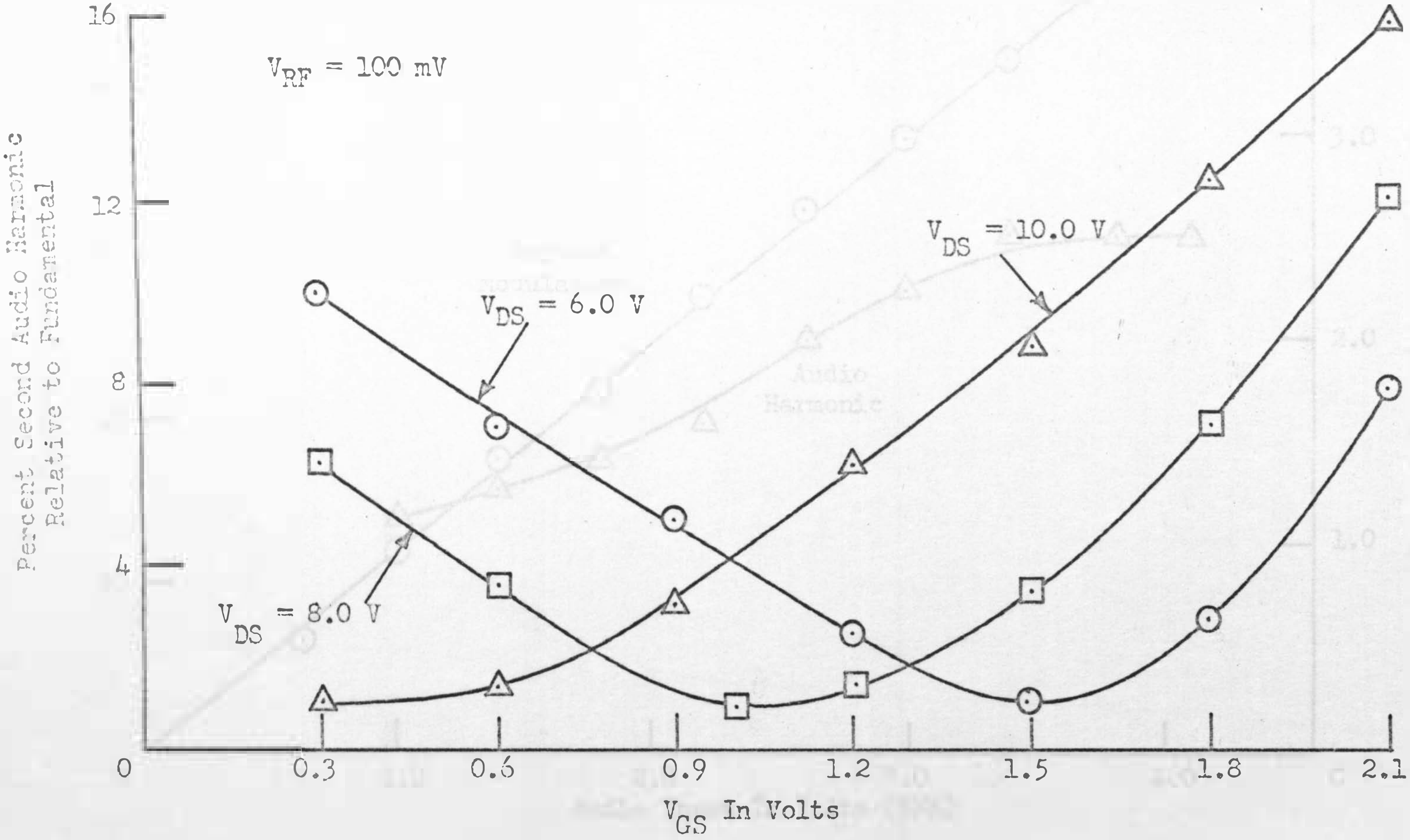

Fig. 18. Sideband distortion as a function of V_{GS}; 100 percent modulation.

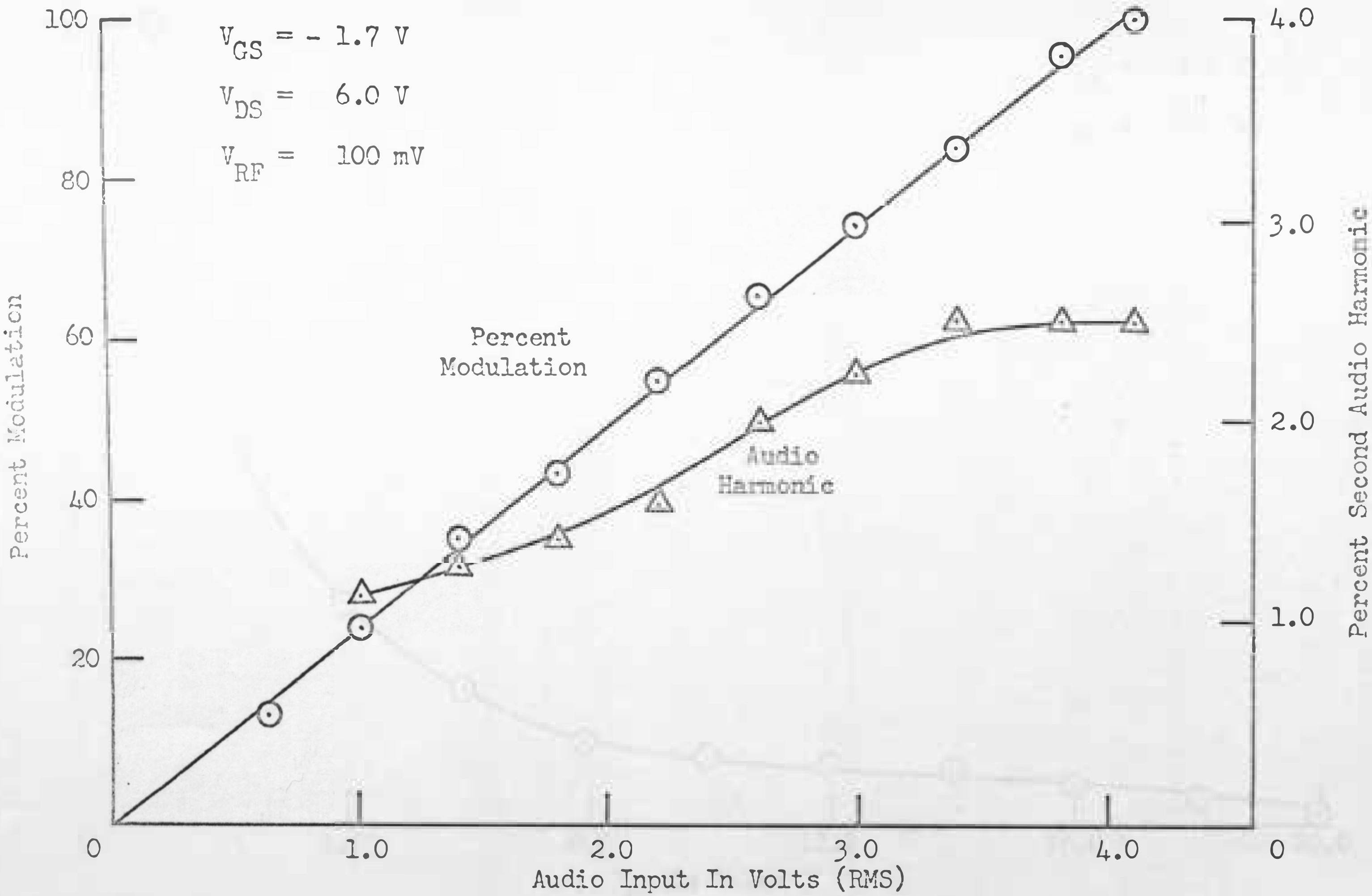

Fig. 19. Variation of percent modulation and sideband distortion with modulating signal amplitude.

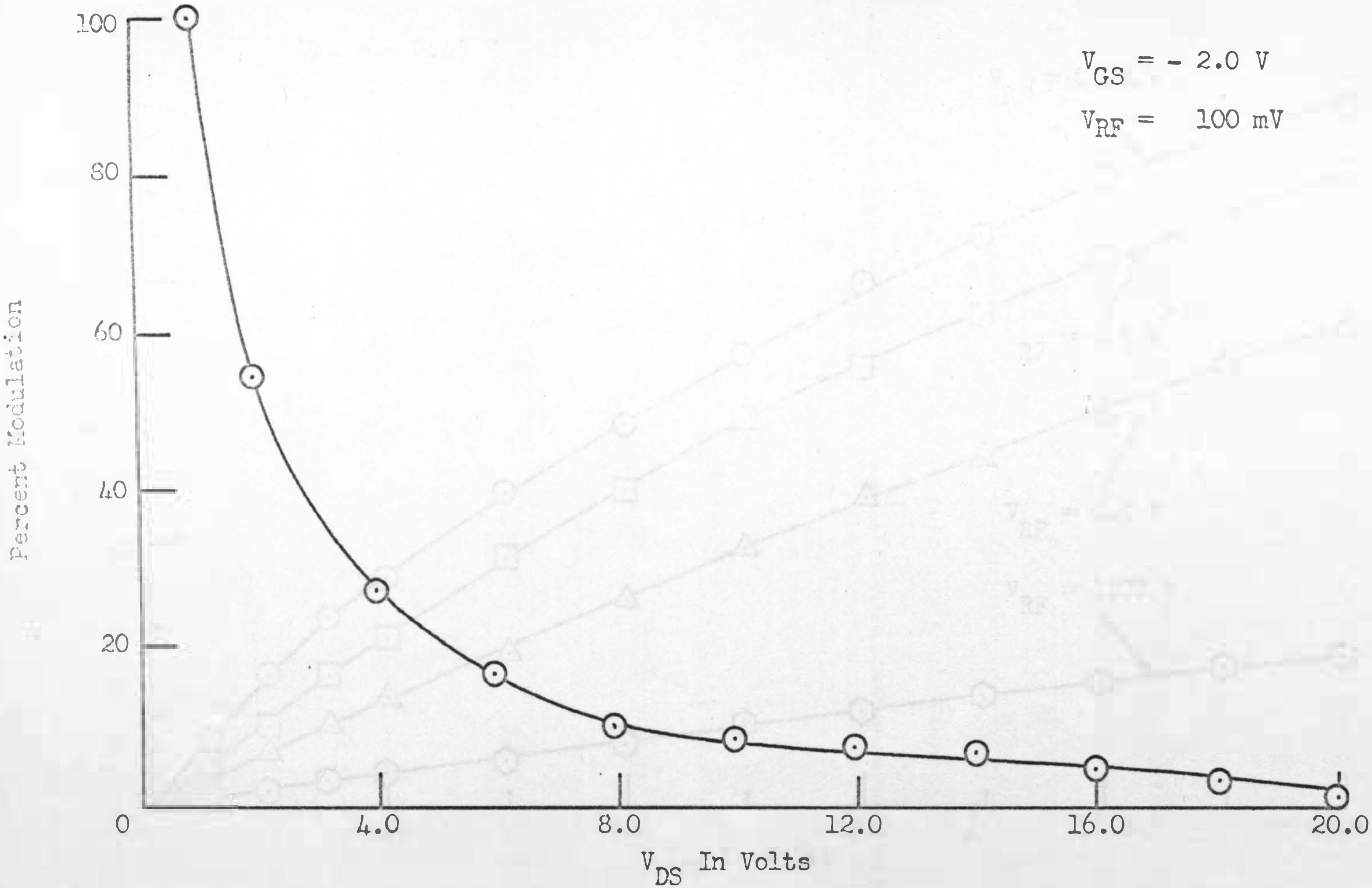

Fig. 20. Variation of percent modulation with V_{DS} for the 2N3823 FET drain modulator.

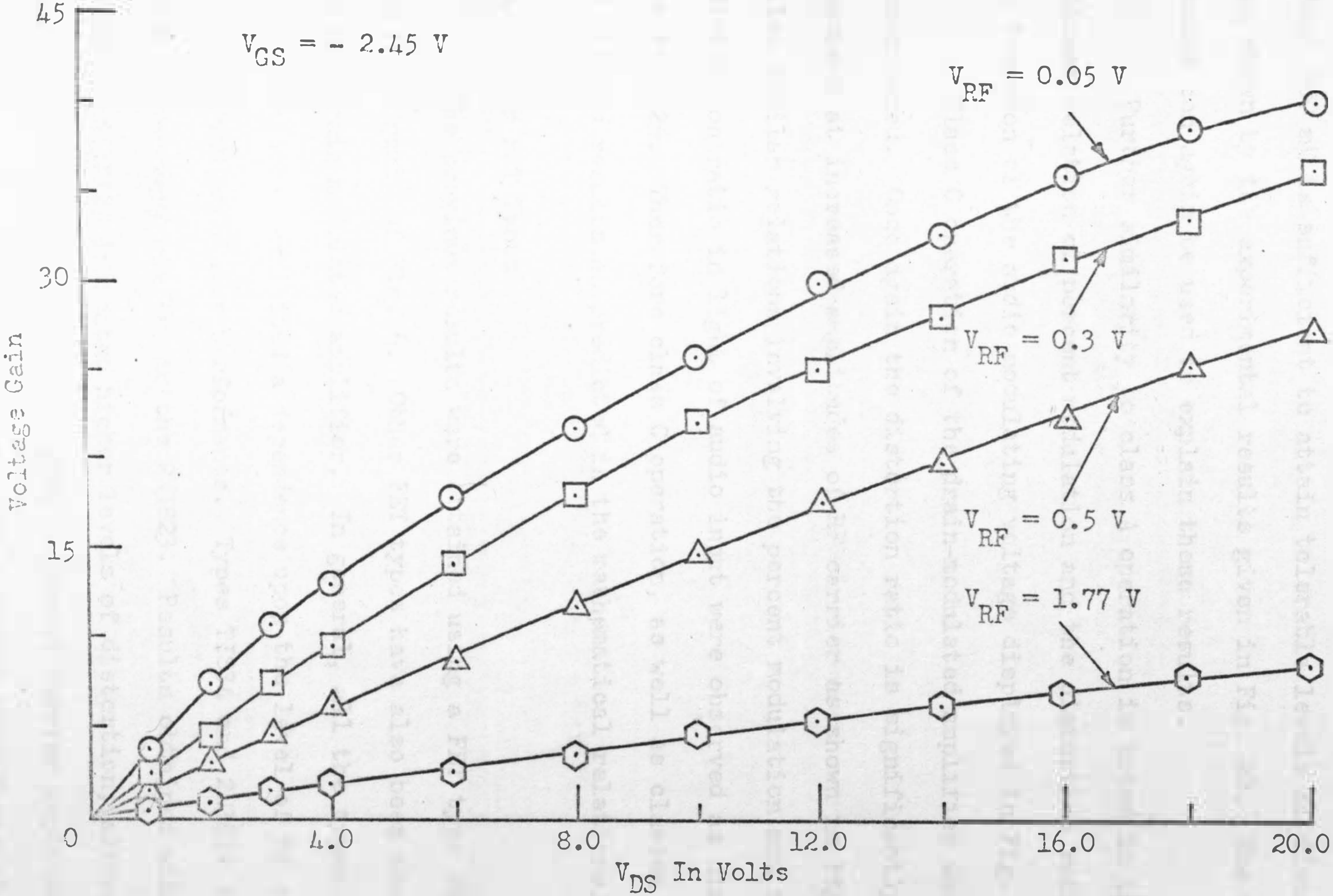

Fig. 21. Effect of carrier amplitude upon voltage gain for class B operation.

desirable modulation characteristic. Further investigation reveals that 300 mV is sufficient to attain tolerable levels of distortion as shown by the experimental results given in Fig. 22. The arctangent model can again be used to explain these results.

Further similarity to class A operation is noted in the near linear relation of percent modulation and the distortion ratio as a function of the audio modulating voltage displayed in Fig. 23.

Class C operation of the drain-modulated amplifier was also considered. Once again the distortion ratio is significantly reduced at increased amplitudes of RF carrier as shown in Fig. 24. Also similar relations involving the percent modulation and the distortion ratio in light of audio input were observed as displayed in Fig. 25. Therefore class C operation, as well as classes A and B, yields results as predicted in the mathematical relations.

D. Other FET Types

The previous results were obtained using a FET type 2N3823 in the circuit of Fig. 6. Other FET types have also been observed in the drain modulated amplifier. In general, all the types that were considered exhibited a dependence upon the level of RF carrier for improved modulator performance. Types TIS34 and 2N3819 behaved in a manner very similar to the 2N3823. Results obtained with types 2N3575 and 3N125 indicated higher levels of distortion; although improvement was still observed with increased carrier amplitude.

In addition to the junction FET a 2N3796 MOSFET was also studied. Once again the straightening effect due to large-signal

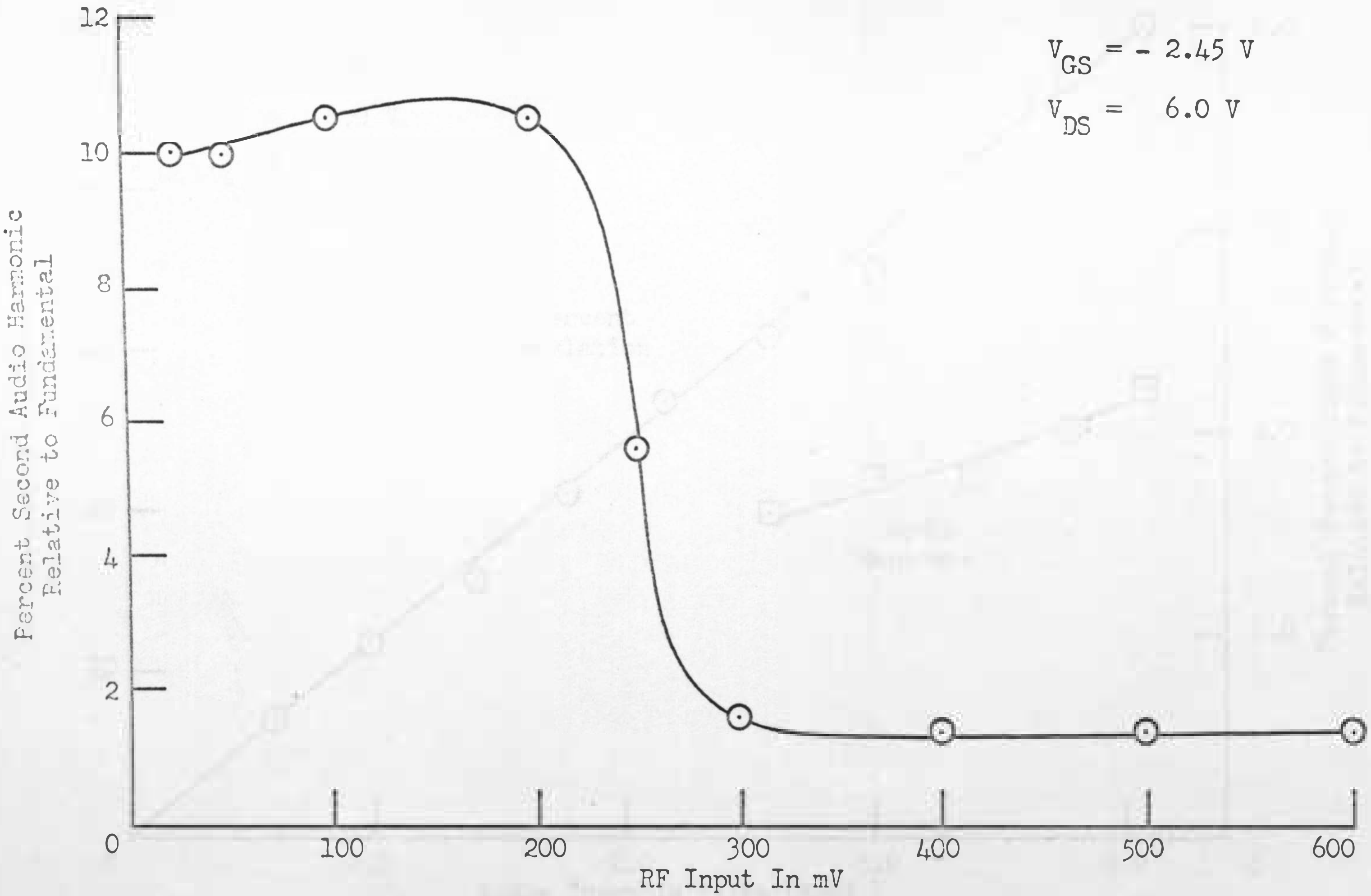

Fig. 22. Variation of sideband distortion with carrier amplitude for 100 percent modulation and class B operation.

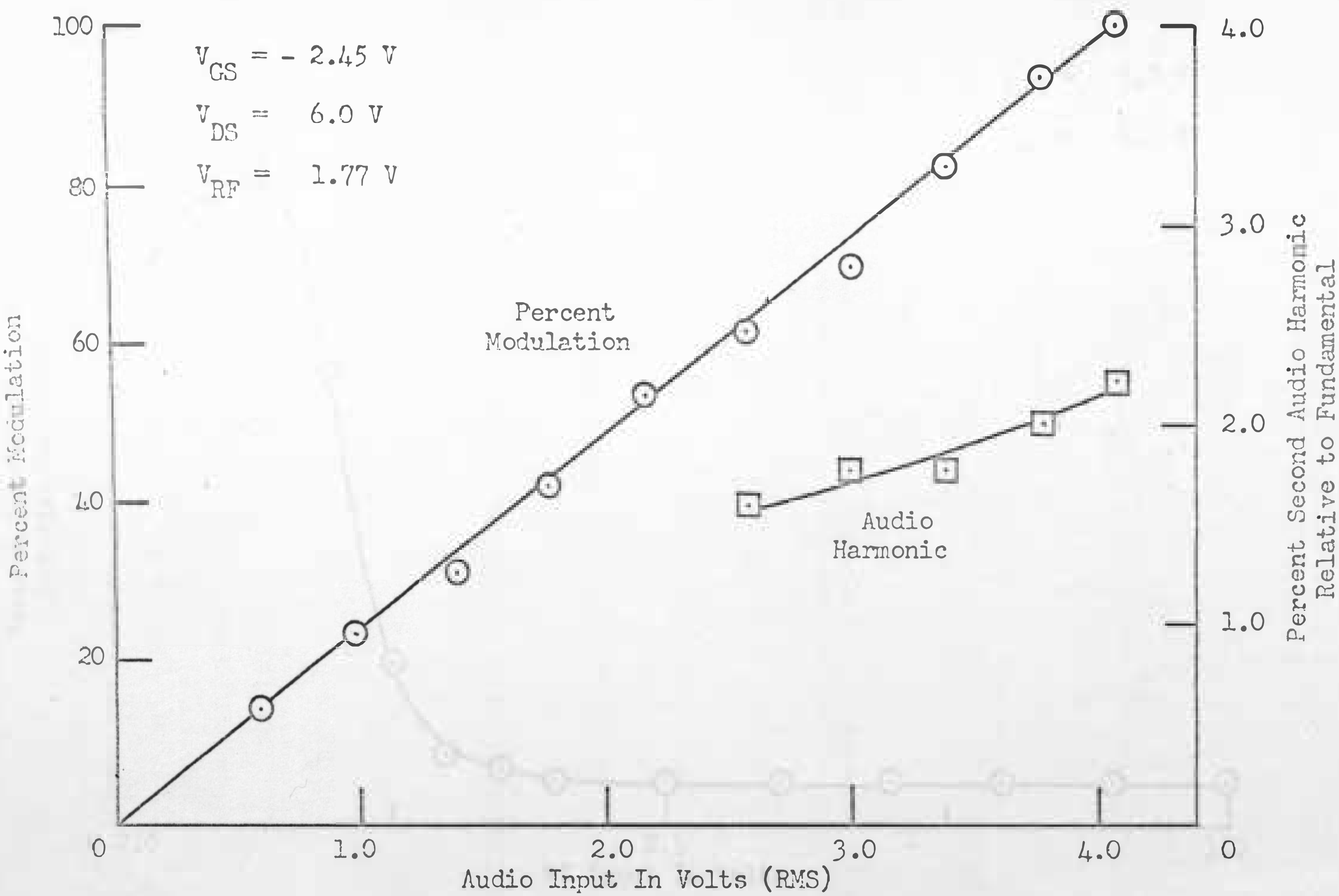

Fig. 23. Sideband distortion and percent modulation as a function of the modulating signal amplitude; class B.

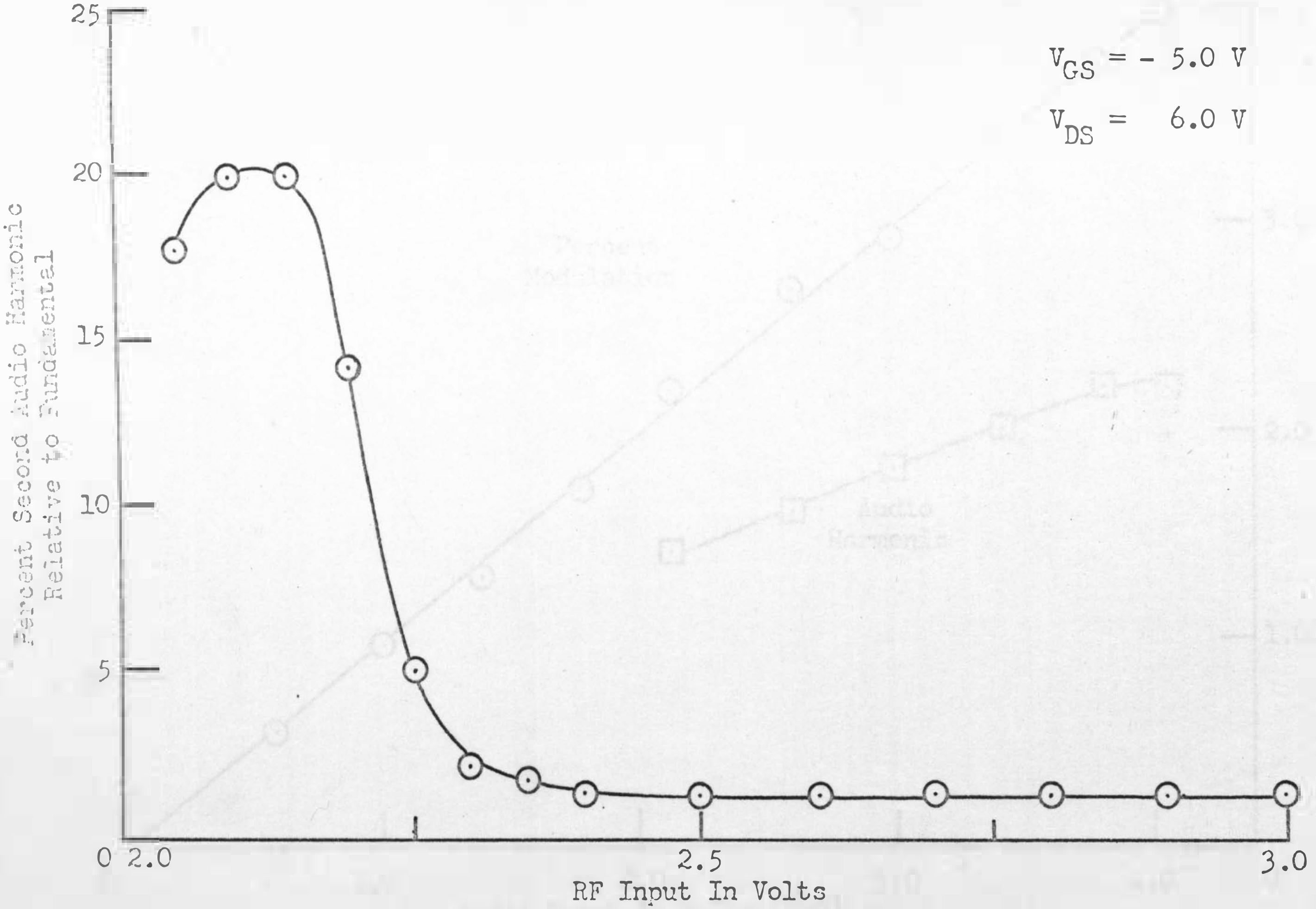

Fig. 24. Variation of sideband distortion with carrier amplitude for 70 percent modulation and class C operation.

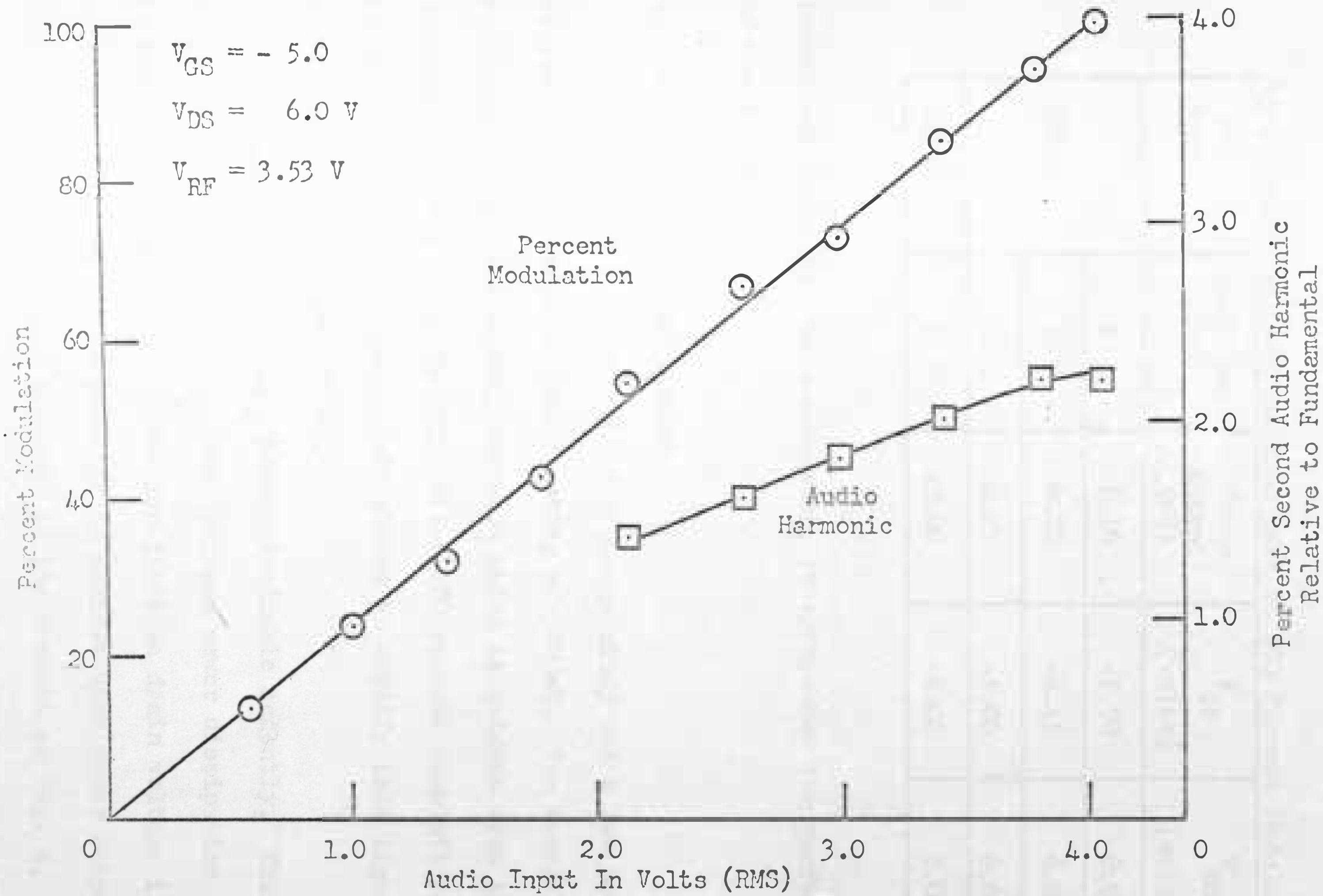

Fig. 25. Sideband distortion and percent modulation as a function of the modulating signal amplitude; class C.

TABLE I

Power Output in the Modulated Wave at 100 Percent Modulation

FET Type	Amplifier Class	Power Output (mW)	V_{GS} (volts)	V_{DS} (volts)
2N3823	A	0.16	-1.70	6.0
	B	0.22	-2.45	6.0
	C	0.21	-5.00	6.0
CP651	A	25.00	-2.00	5.0

inputs was observed. As a modulator, it approached the performance of the 2N3823.

E. Higher Power FET Modulators

The 2N3823 FET used in the previous study was a low power device with a power dissipation rating of 300 mW. The resulting modulated signal was a low power wave which is evident from the experimental data given in Table I for 100 percent modulation. It would be necessary for most applications to amplify this signal before it could be transmitted.

Higher power FETs have become available recently. The type CP651 is an example with a typical maximum power dissipation rating of 8 watts. However, due to the low limit on drain voltage (20 volts maximum), it is not possible to achieve high power outputs. With an effective load of 500 ohms in the circuit of Fig. 6, a power output of 25 mW was achieved as given in Table I. With regard to distortion levels and the percent modulation, this type exhibited characteristics similar to the 2N3823. However distortion levels were a little higher. The dependence of distortion on carrier input, audio input, and V_{DS} followed the pattern displayed by the type 2N3823.

CHAPTER V

CONCLUSIONS

Amplitude modulation can be effectively accomplished by drain-modulating a FET amplifier. Although considerable distortion is introduced at small-signal carrier inputs, this can be reduced by increasing the carrier input to large-signal levels.

Small-signal analysis indicates that r_{ds} is the major contributor to a linear modulation characteristic. The other significant parameter g_m contributes very little due to its virtual saturation at drain voltage levels above the pinch-off region. However, since it is necessary to use large-signal inputs to reduce distortion to tolerable levels, the small-signal parameters cannot be used to completely analyze modulator performance.

The predictions of modulator performance based upon the voltage-transfer ratio as a polynomial in v_{DS} were experimentally supported. Percent modulation exhibited a linear relationship with the modulating signal amplitude, and the audio distortion varied in an approximately linear manner with this quantity. Also, percent modulation was found to vary inversely with V_{DS} as predicted. However, due to an apparent variation in the polynomial coefficients with carrier amplitude, the effect of this parameter cannot be predicted with the polynomial representation. It then becomes necessary to use a model such as an arctangent input-output representation to predict the large-signal effects.

The presently available power FET exhibits the same parameter dependencies as the low-power devices. Therefore, as higher power devices become available, the present study can serve as a basis for analyzing their performance.

In summary, the important considerations for a drain-modulated FET amplifier are as follows:

1. The effective load on the amplifier should be greater than or of the same order of magnitude as the highest encountered values of r_{ds} to minimize distortion.

2. The bandwidth of the amplifier should be at least twice the highest expected modulating frequency.

3. The correct combination of bias voltages for class A operation must be determined experimentally to choose an optimum operating point. This does not apply for amplifier classes B and C.

4. The carrier input should be chosen large enough to reduce the audio harmonic distortion to tolerable levels.

REFERENCES

1. Black, H. S., Modulation Theory, D. Van Nostrand Co., Inc., 1953.

2. Carson, J. R., "Notes on Theory of Modulation", Proc. IRE, Vol. 10, 1922, pp. 57-64.

3. Costas, John P., "Synchronous Communications", Proc. IEEE, Vol. 44, December 1956, pp. 1713-1718.

4. Everitt, W. L. and G. E. Anner, Communication Engineering, McGraw-Hill Book Co., Inc., 1954, pp. 1-43, 249-293.

5. Fitchen, F. C., Transistor Circuit Analysis and Design, D. Van Nostrand Co., Inc., 1966, p. 2.

6. Fitchen, F. C. and J. C. Lietz, "The FET Drain Modulator", Proc. of the National Electronics Conference, Vol. 23, 1967, pp. 226-230.

7. Gaudernack, L. F., "Some Notes on the Practical Measurement of the Degree of Amplitude Modulation", Proc. IRE, Vol. 22, 1934, pp. 819-846.

8. Goldman, Stanford, Frequency Analysis, Modulation, and Noise, McGraw-Hill Book Co., Inc., 1948, pp. 141-204, 215-216.

9. Gottlieb, Irving M., Understanding Amplitude Modulation, Howard W. Sams and Co., Inc., 1966.

10. Gray, Truman S., Applied Electronics, John Wiley & Sons, Inc., 1954, pp. 689-715, 738-754.

11. Hartley, R. V. L., "Relations of Carrier and Sidebands in Radio Transmission", Proc. IRE, Vol. 11, 1923, pp. 34-56.

12. Heising, Raymond A., "Modulation Methods", Proc. IRE, Vol. 50, 1962, pp. 896-901.

13. Krauss, H. L. and J. F. Sanford, "Collector Modulation of Transistor Amplifiers", IEEE Transactions on Circuit Theory, Vol. CT-12, No. 3, 1965, pp. 426-428.

14. Luck, D. G. C. and H. Roder, "Discussion on Amplitude, Phase, and Frequency Modulation", Proc. IRE, Vol. 20, 1932, pp. 884-887.

15. Robinson, H. A., "An Experimental Study of the Tetrode as a Modulated Radio-Frequency Amplifier", Proc. IRE, Vol. 20, 1932, pp. 131-160.

16. Roder, H., "Amplitude, Phase, and Frequency Modulation", Proc. IRE, Vol. 19, 1931, pp. 2145-2176.

17. Tompkins, Jon D., "An Inside Look at FET Terminology and Parameters", Electrical Design News, July 1964, p. 48.

18. Wallmark, J. Torkel and Harwick Johnson, Field-Effect Transistors, Prentice-Hall, Inc., 1966.

APPENDICES

APPENDIX A

ARCTANGENT REPRESENTATION OF THE FET INPUT-OUTPUT CHARACTERISTIC

The arctangent model approximation of the input-output relation is

$$\tan \theta(y + \alpha) = \phi(x + \beta) \tag{A-1}$$

where α and β represent an offset in biasing in the vertical and horizontal directions respectively from the center of the characteristic shown in Fig. 15.

If the arctangent curve is allowed to go to 1.47 radians instead of $\pi/2 = 1.57$ radians, then

$$\theta = \frac{1.47}{a/2} \tag{A-2}$$

where a is the vertical distance between the cutoff and saturation levels in Fig. 15.

For small values of x, and $\alpha = 0$, ϕ is equal to the product of the small-signal gain (A_v) and θ because the tangent of a small number numerically approximates the number. Therefore,

$$\theta y = \phi x \qquad \text{(for small x)}$$

and

$$\phi = \theta\frac{y}{x} = -\,\theta A_v \tag{A-3}$$

For the condition of no signal input,

$$\tan \theta\alpha = \phi\beta$$

$$\beta = \frac{1}{\phi}\tan \theta\alpha \qquad \text{(A-4)}$$

The tangent function in Eq. (A-1) can be represented by a series:

$$\tan \theta(y + \alpha) = \theta(y + \alpha) + \frac{\theta^3(y + \alpha)^3}{3}$$

$$+ \frac{2\theta^5(y + \alpha)^5}{15}$$

$$= k_o + k_1 y + k_2 y^2 + k_3 y^3 + \dots \qquad \text{(A-5)}$$

where

$$k_o = \theta\alpha + \frac{\theta^3\alpha^3}{3} + \frac{2\theta^5\alpha^5}{15}$$

$$k_1 = \theta + \theta^3\alpha^2 + \frac{2\theta^5\alpha^4}{3}$$

$$k_2 = \theta^3\alpha + \frac{4\theta^5\alpha^3}{3}$$

$$k_3 = \frac{\theta^3}{3} + \frac{4\theta^5\alpha^2}{3}$$

If the series

$$y = a + bx + cx^2 + dx^3 + \dots$$

is used to represent the voltage transfer characteristic, a sinusoidal input will yield the following series:

$$y = a_o + a_1 \sin \omega t + a_2 \cos\ 2\omega t + a_3 \sin 3\omega t + \ldots \qquad \text{(A-6)}$$

In series form the trigonometric functions become:

$$\sin \omega t = \omega t - \frac{\omega^3 t^3}{6} + \frac{\omega^5 t^5}{120} - \ldots$$

$$\cos\ 2\omega t = 1 - 2\omega^2 t^2 + \frac{2\omega^4 t^4}{3} - \ldots$$

$$\sin 3\omega t = 3\omega t - \frac{9\omega^3 t^3}{2} + \frac{81\omega^5 t^5}{40} - \ldots$$

Substituting these quantities into Eq. (A-6) results in the following:

$$y = (a_o + a_2) + (a_1 + 3a_3)\omega t + (-2a_2)\omega^2 t^2$$

$$+ \left(-\frac{a_1}{6} - \frac{9a_3}{2}\right)\omega^3 t^3 + \ldots$$

Representing the coefficients with other symbols we have:

$$y = A + B\omega t + C\omega^2 t^2 + D\omega^3 t^3 + \ldots \qquad \text{(A-7)}$$

However the d.c. quantities are accounted for by α and β, so

$$A = a_o + a_2 = 0$$

Inserting the series of Eq. (A-7) with $A = 0$ into Eq. (A-5) and grouping terms gives:

$$\tan \theta(y + \alpha) = k_o + k_1 B\omega t + (k_1 C + k_2 B^2)\omega^2 t^2$$

$$+ (k_1 D + 2k_2 B + k_3 B^3)\omega^3 t^3 + \ldots \qquad \text{(A-8)}$$

Assume a sinusoidal input:

$$x = V\sin \omega t = V(\omega t - \frac{\omega^3 t^3}{6} + \frac{\omega^5 t^5}{120} - \ldots)$$

Using this and Eq. (A-8) in Eq. (A-1) results in the following:

$$k_o + k_1 B\omega t + (k_1 C + k_2 B^2)\omega^2 t^2$$

$$+ (k_1 D + 2k_2 BC + k_3 B^3)\omega^3 t^3 + \ldots$$

$$= \phi V(\omega t - \frac{\omega^3 t^3}{6} + \frac{\omega^5 t^5}{120} - \ldots) + \phi\beta$$

From this relation we find:

$$k_o = \phi\beta$$

$$k_1 B = \phi V$$

$$k_1 C + k_2 B^2 = 0$$

$$k_1 D + 2k_2 BC + k_3 B^3 = -\frac{\phi V}{6}$$

Solving for A, B, C, and D gives the following relations:

$$A = a_o + a_2 = 0$$

$$B = a_1 + 3a_3 = \frac{V}{k_1}$$

$$C = -2a_2 = -\frac{k_2 \phi^2 V^2}{k_1{}^3}$$

$$D = -\frac{a_1}{6} - \frac{9a_3}{2} = -\frac{\phi V}{6k_1} + (\frac{2k_2{}^2 - k_1 k_3}{k_1{}^5})\phi^3 V^3$$

A simultaneous solution of these equations yields the final results:

$$a_o = -\frac{k_2}{2k_1^3}\phi^2V^2$$

$$a_1 = \frac{\phi V}{k_1} + \frac{3}{4}\left(\frac{2k_2^2 - k_1k_3}{k_1^5}\right)\phi^3V^3$$

$$a_2 = \frac{k_2}{2k_1^3}\phi^2V^2$$

$$a_3 = -\left(\frac{2k_2^2 - k_1k_3}{4k_1^5}\right)\phi^3V^3$$

These are the coefficients of the harmonic components in the output wave as given in Eq. (A-6).

Computer Solution of the Harmonic Coefficients in FORTRAN

```
11 FORMAT (13HE.E. RESEARCH)
10 FORMAT (21HLARGE SIGNAL ANALYSIS//)
12 FORMAT (4E12.4)
13 FORMAT (2HA=,E12.4,2X,2HG=,E12.4,2X,3HRL=,E12.4,2X,4HVDD=,E12.4)
14 FORMAT (3HDI=,E12.4,2X,3HAO=,E12.4,2X,4HA11=,E12.4,2X,4HA13=,
         E12.4)
15 FORMAT (3HA2=,E12.4,2X,3HA3=,E12.4//)
   PUNCH 11
   PUNCH 10
 1 READ 12,A,G,RL,VDD
   PUNCH 13,A,G,RL,VDD
```

```
2 DO 3 I=1,65,2
  W=I-1
  DI=W*.0001
  DIC=VDD/(2.*RL)
  AL=(DIC-DI)*RL
  TH=1.47/(A/2.)
  PHI=G*TH
  BETA=(1./PHI)*SINF(TH*AL)/COSF(TH*AL)
  X=TH**3
  Y=TH**5
  Z=AL**2
  ZZ=Z*AL
  ZZZ=ZZ*AL
  ZZZZ=ZZZ*AL
  DO=TH*AL+X*ZZ/3.+Y*ZZZZ*(a./15.)
  D1=TH+X*Z+Y+ZZZ*(2./3.)
  D2=X*AL+(4./3.)*Y*ZZ
  D3=X/3.+Y*Z*(4./3.)
  TU=D1**3
  TS=TU*D1
  TT=TS*D1
  PH3=PHI**3
  DEL=(2.*(D2**2)*PH3-D1*D3*PH3)/TT
  AO=-D2*(PHI**2)/(2.*TU)
  A11=PHI/D1
```

```
      A13=(.75)*DEL
      A2=-AO
      A3=-DEL/4.
      PUNCH 14,DI,AO,A11,A13
    3 PUNCH 15,A2,A3
      GO TO 1
      END
```

Data Card:

16.0000E+00 04.0000E+00 25.0000E+02 16.0000E+00

Definitions of Terms:

A = a

G = small-signal gain

RL = load impedance

VDD = drain bias supply

DI = drain current

AO = a_o

A11 = coefficient of V in the relation for a_1

A13 = coefficient of V^3 in the relation for a_1

A2 = coefficient of V^2 in the second harmonic relation for a_2

A3 = coefficient of V^3 in the third harmonic relation for a_3

APPENDIX B

CARRIER SUPPRESSOR

The amplitude of the carrier frequency component in an amplitude modulated wave is always at least twice as great as any sideband frequency. This reduces the sensitivity of a spectrum analyzer when attempting to measure the sideband amplitudes, particularly if they are small relative to the carrier. It would be desirable to reduce the amplitude of the carrier so greater sensitivity could be obtained.

The network shown in Fig. 26 was used to suppress the carrier frequency while passing the sideband frequencies unaffected relative to one another. The carrier input wave of the modulated amplifier and the modulated output wave are introduced at the designated points. Since the carrier frequencies at the input and output of the common-source amplifier are 180 degrees different in phase, the two signals subtract in this network resulting in a reduced carrier amplitude. Because the sideband frequencies are present in only one of the signals, they are unaffected. Adjustment of the 100 KΩ variable resistor allows an optimum suppression to be obtained. The particular circuit components were chosen experimentally for best operation.

The performance of the suppression network was checked by taking measurements on the modulated wave with and without the network at a level of modulation where the carrier did not interfere with sideband measurements. The results of this test are given in Table II. No variations were noted between the two measurements. It was concluded that this network would not affect measurements on the sideband frequencies.

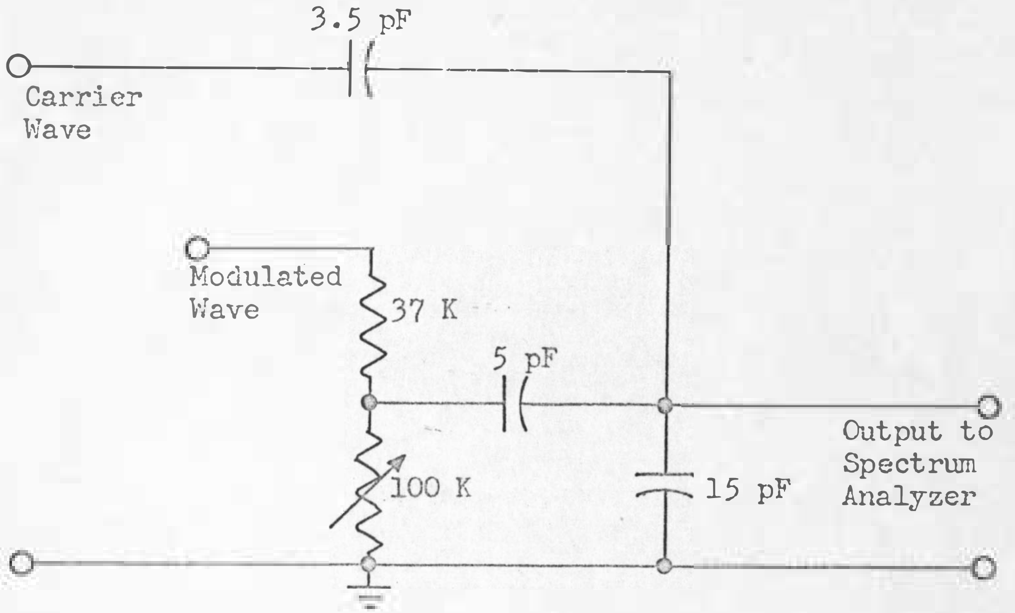

Fig. 26. Carrier suppressor circuit used in conjunction with the spectrum analyzer.

TABLE II

Harmonic Suppressor Test Data

Bias Voltage		Audio Input (volts)	Without Suppressor		With Suppressor	
V_{GS}	V_{DS}		Second Harmonic (db)	Third Harmonic (db)	Second Harmonic (db)	Third Harmonic (db)
- 2.45	6.0	4.0	- 6	- 33	- 6	- 33
		3.5	- 9	- 34	- 9	- 34
		3.0	- 10	- 35	- 10	- 35
		2.5	- 12	- 36	- 12	- 36

Note: Decibel measurements were made with respect to the fundamental sideband frequency.